

Fast Model Selection and Stable Optimization for Softmax-Gated Multinomial-Logistic Mixture of Experts Models

TrungKhang Tran ^{*1} TrungTin Nguyen ^{*23} Md Abul Bashar ²³ Nhat Ho ⁴ Richi Nayak ²³
 Christopher Drovandi ²³

Abstract

Mixture-of-Experts (MoE) architectures combine specialized predictors through a learned gate and are effective across regression and classification, but for classification with softmax multinomial-logistic gating, rigorous guarantees for stable maximum-likelihood training and principled model selection remain limited. We address both issues in the full-data (batch) regime. First, we derive a batch minorization-maximization (MM) algorithm for softmax-gated multinomial-logistic MoE using an explicit quadratic minorizer, yielding coordinate-wise closed-form updates that guarantee monotone ascent of the objective and global convergence to a stationary point (in the standard MM sense), avoiding approximate M-steps common in EM-type implementations. Second, we prove finite-sample rates for conditional density estimation and parameter recovery, and we adapt dendograms of mixing measures to the classification setting to obtain a sweep-free selector of the number of experts that achieves near-parametric optimal rates after merging redundant fitted atoms. Experiments on biological protein–protein interaction prediction validate the full pipeline, delivering improved accuracy and better-calibrated probabilities than strong statistical and machine-learning baselines.

1. Introduction

1.1. Mixture of Experts Models

Mixture of experts (MoE) models (Jacobs et al., 1991; Jordan & Jacobs, 1994) represent heterogeneous predictor–response relationships by combining a *gating* model with multiple *expert* models, both depending on the input. The gate assigns input-dependent weights to experts, enabling conditional computation (Bengio, 2013; Chen et al., 2022) and inducing a data-adaptive partition of the input domain. In classification, softmax-gated multinomial-logistic MoE (SGMLMoE) (Chen et al., 1999; Yuksel & Gader, 2010; Huynh & Chamroukhi, 2019; Pham & Chamroukhi, 2022; Nguyen et al., 2024a) offer calibrated multiclass probabilities while retaining the conditional-computation benefits of gating. MoE theory is supported by approximation and estimation guarantees in several regimes, including classical mixtures (Genovese & Wasserman, 2000; Rakhlin et al., 2005; Nguyen, 2013; Ho & Nguyen, 2016a;b; Nguyen et al., 2020b; 2022b; Chong et al., 2024), mixtures of regressions (Do et al., 2025; Ho et al., 2022), and broader MoE frameworks (Jiang & Tanner, 1999b; Nguyen et al., 2024c; Norets, 2010; Nguyen et al., 2016; 2019; 2021a; 2023a; 2024a;b); see also surveys (Yuksel et al., 2012; Masoudnia & Ebrahimpour, 2014; Nguyen & Chamroukhi, 2018; Nguyen, 2021; Cai et al., 2025). Despite this progress, for SGMLMoE two core issues remain underdeveloped: *stable* maximum-likelihood training with provable convergence, and *model selection* (especially the number of experts) with rigorous guarantees and computational efficiency.

1.2. Stable Maximum-likelihood Training via MM in the Full-data Regime

Likelihood-based estimation for SGMLMoE is challenging because the observed-data objective couples softmax gating and multinomial-logistic experts in a highly non-convex way. EM (Dempster et al., 1977; Meilijson, 1989; McLachlan & Krishnan, 1997) is the classical template for latent-variable models, but in multinomial-logistic MoE the M-steps typically lack closed forms, so practical EM relies on inner-loop or approximate maximization, which can complicate

^{*}Co-first Author. ¹School of Computing, National University of Singapore, Singapore. ²ARC Centre of Excellence for the Mathematical Analysis of Cellular Systems. ³School of Mathematical Sciences, Queensland University of Technology, Brisbane, Australia. ⁴Department of Statistics and Data Science, University of Texas at Austin, Austin, USA. Correspondence to: TrungTin Nguyen <t600.nguyen@qut.edu.au>.

monotonicity and global convergence guarantees. MM algorithms (Ortega & Rheinboldt, 1970; De Leeuw, 1977; De Leeuw & Heiser, 1977; Lange, 2016; Sun et al., 2017; Nguyen, 2017; Lange et al., 2021; Mairal, 2015; 2013) instead optimize explicit surrogates that majorize/minorize the objective and can yield simple updates with stability guarantees. We focus on the *batch* regime, avoiding the stochastic-approximation noise inherent in incremental and mini-batch variants of EM/MM (Borkar, 2008; Kushner & Yin, 2003; Dieuleveut et al., 2023; Fort & Moulaines, 2023; Wang et al., 2019; Cappé & Moulaines, 2009; Cappé, 2011; Fort et al., 2021a; 2020; Nguyen et al., 2020a; Kuhn et al., 2020; Karimi et al., 2019b; Corff & Fort, 2013; Karimi et al., 2019a; Oudoumanessah et al., 2024; 2025; Chen et al., 2018; Fort et al., 2021b; Fort & Moulaines, 2021) and related variational/free-energy views (Neal & Hinton, 1998).

1.3. Model Selection in SGMLMoE Models

Selecting the number of experts remains central. Classical criteria require fitting multiple model sizes and then applying AIC (Akaike, 1974; Frühwirth-Schnatter et al., 2018), BIC (Schwarz, 1978; Khalili et al., 2024; Forbes et al., 2022a; Berrettini et al., 2024; Forbes et al., 2022b; Nguyen & Nguyen, 2025; Ho et al., 2025), ICL (Biernacki et al., 2000; Frühwirth-Schnatter et al., 2012), eBIC (Foygel & Drton, 2010; Nguyen & Li, 2024), or SWIC (Sin & White, 1996; Westerhout et al., 2024). For MoE, over-specification can induce non-identifiability and singularities, undermining the usual asymptotic justifications. Alternatives include non-asymptotic penalization (Nguyen et al., 2021b; 2022a;c; 2023b; Montuelle & Le Pennec, 2014; Nguyen et al., 2023c) and Bayesian/post-processing strategies such as merge-truncate-merge (Frühwirth-Schnatter, 2019; Zens, 2019; Guha et al., 2021; Nguyen et al., 2024d), but many remain tied to multi- K sweeps. A recent sweep-free direction uses dendrograms of mixing measures (Do et al., 2024; Thai et al., 2025; Hai et al., 2026), developed mainly for Gaussian-expert settings; we adapt this viewpoint to multinomial-logistic classification and integrate it with stable batch-MM training.

1.4. Contributions and Paper Organization

We develop a unified framework for SGMLMoE that couples *stable batch maximum-likelihood training* with *sweep-free model selection*. On the optimization side, we construct an explicit quadratic MM surrogate, leading to coordinate-wise closed-form updates that exactly minimize the surrogate each iteration and therefore guarantee monotone ascent and global convergence to a stationary point without inner-loop M-steps. On the statistical side, we establish finite-sample rates for conditional density estimation and parameter recovery, and we introduce a dendrogram-based aggregation path on mixing measures that restores near-

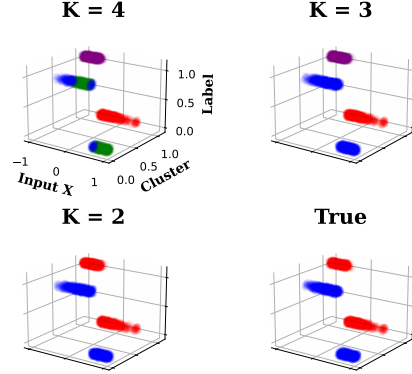


Figure 1. Illustration of the DSC merging path on an over-specified fit ($K = 4, M = 2$): successive merges remove near-duplicate experts and recover the true expert structure ($K_0 = 2, M = 2$).

parametric rates after merging redundant fitted atoms (see Table 1) and yields a consistent order selector without multi- K training (see Figure 1).

Organization. Section 2 introduces SGMLMoE and the likelihood objective. Section 3 presents the batch MM algorithm and its monotonicity. Section 4 develops the Voronoi loss, aggregation path, convergence rates, and dendrogram selection criterion. Experiments are reported in Section 5. All additional technical proofs and implementation details are deferred to the appendix.

2. Preliminaries

SGMLMoE Models. We refer to the output $y \in \mathbb{Y}$ as the response variable and the input $\mathbf{x} \in \mathbb{X} \subset \mathbb{R}^P, P \in \mathbb{N}$, as the predictor variable. We consider a batch dataset of size N , denoted by $\{(\mathbf{x}_n, y_n) : n \in [N]\}$, consisting of i.i.d. copies of (\mathbf{x}, y) , where the conditional law of y given $\mathbf{x} = \mathbf{x}$ is characterized by an unknown conditional probability mass function (or density) $\pi(\cdot | \mathbf{x} = \mathbf{x})$. The corresponding observed values are written as (\mathbf{x}, y) . Motivated by universal approximation results for MoE models, we approximate $\pi(\cdot | \mathbf{x} = \mathbf{x})$ by a SGMLMoE of the form

$$s_{\theta}(y | \mathbf{x}) = \sum_{k=1}^K g_k(\mathbf{w}(\mathbf{x})) e_k(y; \mathbf{v}(\mathbf{x})), \quad (1)$$

where θ collects all unknown parameters and K is the number of experts. The gating probabilities are defined by the softmax map $g_k(\mathbf{w}(\mathbf{x})) = \exp(w_k(\mathbf{x})) / (\sum_{l=1}^K \exp(w_l(\mathbf{x})))$, $\forall k \in [K]$, with gating score functions $\mathbf{w}(\mathbf{x}) = (w_1(\mathbf{x}), \dots, w_K(\mathbf{x}))$. In the discrete-output setting, we take $\mathbb{Y} = [M]$, $M \in \mathbb{N}$, and specify each expert as a multinomial-logistic model $e_k(y = m; \mathbf{v}(\mathbf{x}; \mathbf{v})) = \exp(v_{m,k}(\mathbf{x})) / \sum_{l=1}^M \exp(v_{l,k}(\mathbf{x}))$, $\forall k \in [K]$, $\forall m \in [M]$, where the expert scores $\mathbf{v}(\mathbf{x}) =$

$(v_{m,k}(\mathbf{x}))_{m \in [M], k \in [K]}$ are modeled as polynomial functions of \mathbf{x} . Concretely, for degrees $D_W, D_V \in \mathbb{N}$, $w_k(\mathbf{x}) = \sum_{d=0}^{D_W} \omega_{k,d}^\top \mathbf{x}^d = \sum_{d=0}^{D_W} \left(\sum_{p=1}^P \omega_{k,d,p} x_p^d \right)$, $v_{m,k}(\mathbf{x}) = \sum_{d=0}^{D_V} \mathbf{v}_{m,k,d}^\top \mathbf{x}^d = \sum_{d=0}^{D_V} \left(\sum_{p=1}^P v_{m,k,d,p} x_p^d \right)$ with coefficient collections $\boldsymbol{\omega} = (\omega_{k,d,p})_{k \in [K], d \in \{0, \dots, D_W\}, p \in [P]}$ and $\mathbf{v} = (v_{m,k,d,p})_{m \in [M], k \in [K], d \in \{0, \dots, D_V\}, p \in [P]}$. The full parameter vector is denoted by $\boldsymbol{\theta} = (\boldsymbol{\omega}, \mathbf{v})$. For simplify, we take $D_W = D_V = D$ and leave the general case $D_W \neq D_V$ for future work.

Maximum Log-likelihood Estimator. We denote by $\boldsymbol{\theta}^0$ a maximizer of the population objective $\boldsymbol{\theta} \mapsto \mathbb{E}_{y|\mathbf{x} \sim \mathbb{P}} [\log s_{\boldsymbol{\theta}}(y | \mathbf{x})]$. Given the batch dataset $\{(\mathbf{x}_n, y_n)\}_{n=1}^N$, we estimate $\boldsymbol{\theta}$ by maximum likelihood, $\hat{\boldsymbol{\theta}}_N \in \arg \max_{\boldsymbol{\theta} \in \mathbb{T}} \frac{1}{N} \mathcal{L}(\boldsymbol{\theta})$, where the observed-data log-likelihood is

$$\mathcal{L}(\boldsymbol{\theta}) = \sum_{n=1}^N \log \left[\sum_{k=1}^K g_k(\mathbf{w}(\mathbf{x}_n)) e_k(y_n; \mathbf{v}(\mathbf{x}_n)) \right]. \quad (2)$$

In this paper we work in the full-data (batch) regime, focusing on stable maximum-likelihood fitting for Equation (1)–Equation (2) without invoking stochastic-approximation devices used in incremental or mini-batch variants.

Identifiability of SGMLMoE Models. Because the softmax gate is invariant to additive shifts, the gating parameters are not fully identifiable. In particular, if we translate each coefficient vector as $\omega_{k,d} \mapsto \omega_{k,d} + \mathbf{t}$ for some $\mathbf{t} \in \mathbb{R}^P$, then the resulting gating probabilities $g_k(\mathbf{w}(\mathbf{x}))$ remain unchanged, so $\{\omega_{k,d}\}$ are identifiable only up to a common translation. This phenomenon, and standard remedies for it, are discussed in the context of establishing convergence rates for maximum-likelihood estimation of softmax-gated Gaussian MoE models in (Nguyen et al., 2023a). Following (Hennig, 2000; Jiang & Tanner, 1999a), we enforce identifiability by fixing a reference expert and imposing, without loss of generality, the constraint $\{\omega_{K,d,p}\}_{d \in \{0, \dots, D\}, p \in [P]} = \mathbf{0}$, which yields the equivalent parameterization $g_K(\mathbf{x}; \boldsymbol{\omega}) = 1 - \sum_{k=1}^{K-1} g_k(\mathbf{x}; \boldsymbol{\omega})$ and $g_k(\mathbf{x}; \boldsymbol{\omega}) = \exp(w_k(\mathbf{x}; \boldsymbol{\omega})) / \left(1 + \sum_{l=1}^{K-1} \exp(w_l(\mathbf{x}; \boldsymbol{\omega})) \right)$ for all $k \in [K-1]$. In addition to the gating identifiability constraint, we also impose an identifiability convention for the multinomial-logistic expert networks, as considered in the convergence-rate analysis for softmax-gated multinomial logistic MoE models in (Nguyen et al., 2024a). Specifically, we fix a reference class and set, without loss of generality, $\{v_{M,k,d,p}\}_{d \in \{0, \dots, D\}, p \in [P]} = \mathbf{0}$ for all $k \in [K]$, so that the last class probability is determined by the remaining $M-1$ logits. Equivalently, for each expert k , we have $e_k(\mathbf{v}_{M,k}(\mathbf{x})) = 1 - \sum_{m=1}^{M-1} e_k(\mathbf{v}_{m,k}(\mathbf{x}))$ and $e_k(\mathbf{v}_{m,k}(\mathbf{x})) =$

$$\exp(v_{m,k}(\mathbf{x})) / \left(1 + \sum_{l=1}^{M-1} \exp(v_{l,k}(\mathbf{x})) \right) \quad \text{for all } m \in [M-1].$$

3. MM Algorithm for SGMLMoE Models

We now specialize the MM framework to the full-data (batch) maximum-likelihood problem for the SGMLMoE model in Equation (1) with discrete output $y \in \mathbb{Y} = [M]$. Let $\{(\mathbf{x}_n, y_n)\}_{n \in [N]}$ be i.i.d. copies of (\mathbf{x}, y) and recall the observed-data log-likelihood $\mathcal{L}(\boldsymbol{\theta})$ in Equation (2). For each datum $n \in [N]$ and expert $k \in [K]$, define the usual posterior responsibility at the current iterate $\boldsymbol{\theta}^{(t)}$ by

$$\tau_{n,k}^{(t)} = \frac{g_k(\mathbf{w}^{(t)}(\mathbf{x}_n)) e_k(\mathbf{v}_{y_n}^{(t)}(\mathbf{x}_n))}{\sum_{l=1}^K g_l(\mathbf{w}^{(t)}(\mathbf{x}_n)) e_l(\mathbf{v}_{y_n}^{(t)}(\mathbf{x}_n))}. \quad (3)$$

To simplify notation for polynomial features, let

$$\hat{\mathbf{x}}_n = [x_{n,1}^0, \dots, x_{n,1}^D, \dots, x_{n,P}^0, \dots, x_{n,P}^D]^\top \in \mathbb{R}^{P(D+1)}.$$

Next, we use an indicator polynomial $\mathbb{1}(z, l)$ to encode class labels: $\mathbb{1}(z, l) = \frac{\prod_{q=1}^M (z-q)}{(z-l)(z-1)!(M-z)!(-1)^{M-z}}$, $\forall z, l \in [M]$, so that $\mathbb{1}(z, l) \in \{0, 1\}$. This representation is convenient for coding and yields the identity $v_{m,k}(\mathbf{x}) = \sum_{l=1}^M \mathbb{1}(m, l) v_{l,k}(\mathbf{x})$, which allows recovering any class logit from the vector of logits.

Batch Sufficient-statistics Notation. For each $n \in [N]$, define the gating-design vector in $\mathbb{R}^{(K-1)P(D+1)}$:

$$\mathbf{s}_n^{(t)} = [\tau_{n,1}^{(t)} x_{n,1}^0, \dots, \tau_{n,1}^{(t)} x_{n,1}^D, \dots, \tau_{n,K-1}^{(t)} x_{n,P}^D]^\top, \quad (4)$$

and define the expert-design vector $\mathbf{r}_n^{(t)}$ by stacking $r_{n,d,l,p,k}^{(t)} = \mathbb{1}(y_n, l) \tau_{n,k}^{(t)} x_{n,p}^d$, $d \in \{0, \dots, D\}$, $l \in [M]$, $p \in [P]$, $k \in [K]$, into $\mathbf{r}_n^{(t)} = [r_{n,0,1,1,1}^{(t)}, \dots, r_{n,D,1,1,1}^{(t)}, \dots, r_{n,D,M,1,1}^{(t)}, \dots, r_{n,D,M,P,K}^{(t)}]^\top$. We also define the class-parameter blocks for each expert k by $\mathbf{c}_k = [v_{1,k,0,1}, \dots, v_{1,k,D,1}, \dots, v_{M,k,D,1}, \dots, v_{M,k,D,P}]^\top$, $\mathbf{v} = \text{vec}([\mathbf{c}_1, \dots, \mathbf{c}_K])$. Finally, we aggregate the batch statistics as $\mathbf{s}^{(t)} = \sum_{n=1}^N \mathbf{s}_n^{(t)}$, $\mathbf{r}^{(t)} = \sum_{n=1}^N \mathbf{r}_n^{(t)}$.

Quadratic Majorizers for the Gate and Experts. For $k \in [K-1]$, let $w_k(\mathbf{x}) = \sum_{d=0}^D \omega_{k,d}^\top \mathbf{x}^d$ and define the gate log-sum-exp term $g_n(\mathbf{w}) = \log \left(1 + \sum_{k=1}^{K-1} \exp(w_k(\mathbf{x}_n)) \right)$. For experts, define for each $k \in [K]$ the multinomial log-sum-exp term $e_n(\mathbf{c}_k) = \log \left(1 + \sum_{m=1}^{M-1} \exp(v_{m,k}(\mathbf{x}_n)) \right)$. For any $K \in \mathbb{N}$, we use the quadratic majorizers based on the matrices

$$\mathbf{B}_{n,K} = \left(\frac{3}{4} \mathbf{I}_{K-1} - \frac{\mathbf{1}_{K-1} \mathbf{1}_{K-1}^\top}{2(K-1)} \right) \otimes \hat{\mathbf{x}}_n \hat{\mathbf{x}}_n^\top. \quad (5)$$

Algorithm 1 Batch MM algorithm for SGMLMoE

Require: Data $\{(\mathbf{x}_n, \mathbf{y}_n)\}_{n=1}^N$; (K, M) ; degree D ; init. $\boldsymbol{\theta}^{(0)} = (\mathbf{w}^{(0)}, \mathbf{v}^{(0)})$; tol. ε ; max iters T .

Ensure: $\{\boldsymbol{\theta}^{(t)}\}_{t \geq 0}$.

- 1: **for** $t = 0, 1, \dots, T-1$ **do**
- 2: **E-step.** For each $n \in [N]$, compute responsibilities $\{\tau_{n,k}^{(t)}\}_{k \in [K]}$ by Equation (3).
- 3: Form sufficient-statistics $\mathbf{s}^{(t)} = \sum_n \mathbf{s}_n^{(t)}$ and $\mathbf{r}^{(t)} = \sum_n \mathbf{r}_n^{(t)}$ using Equation (4) and the definition of $\mathbf{r}_n^{(t)}$ (with $\mathbb{1}(\mathbf{y}_n, l)$).
- 4: Build curvature matrices $\mathbf{B}_{n,K-1} = \sum_n \mathbf{B}_{n,K}$ and $\mathbf{B}_{n,M-1} = \sum_n \mathbf{B}_{n,M}$ with blocks $\mathbf{B}_{n,K}, \mathbf{B}_{n,M}$ from Equation (5).
- 5: Compute $\nabla g(\mathbf{w}^{(t)}) = \sum_n \nabla g_n(\mathbf{w}^{(t)})$ and the expert log-sum-exp gradients $\{\nabla e_n(\mathbf{v}^{(t)})\}_{n \in [N]}$ (definitions in Equation (6)).
- 6: **M-step.** Update (\mathbf{w}, \mathbf{v}) by the closed-form minimizers of the surrogate $\mathcal{S}(\boldsymbol{\theta}, \boldsymbol{\theta}^{(t)})$ in Equation (6): $\mathbf{w}^{(t+1)} = \mathbf{w}^{(t)} + \mathbf{B}_{n,K-1}^{-1} \left(\mathbf{s}^{(t)} - \nabla g(\mathbf{w}^{(t)}) \right)$, $\mathbf{v}^{(t+1)} = \arg \min_{\mathbf{v}} \mathcal{S}((\mathbf{w}^{(t+1)}, \mathbf{v}), \boldsymbol{\theta}^{(t)})$, where the explicit block-linear solve for $\mathbf{v}^{(t+1)}$ is given in Appendix B.
- 7: Set $\boldsymbol{\theta}^{(t+1)} = (\mathbf{w}^{(t+1)}, \mathbf{v}^{(t+1)})$.
- 8: **Stop.** If $|\mathcal{L}(\boldsymbol{\theta}^{(t+1)}) - \mathcal{L}(\boldsymbol{\theta}^{(t)})| \leq \varepsilon$, break.
- 9: **end for**

For compactness, introduce the centered increments $\bar{\mathbf{w}}_t = \mathbf{w} - \mathbf{w}^{(t)}$ and $\bar{\mathbf{c}}_{k,t} = \mathbf{c}_k - \mathbf{c}_k^{(t)}$.

Theorem 1 (Surrogate for the batch negative log-likelihood.). *The following bound defines a batch MM surrogate for $-\mathcal{L}(\boldsymbol{\theta})$, with proof deferred to Section D.2:*

$$-\mathcal{L}(\boldsymbol{\theta}) \leq C^{(t)} + \mathcal{S}_1(\boldsymbol{\theta}, \boldsymbol{\theta}^{(t)}) + \mathcal{S}_2(\boldsymbol{\theta}, \boldsymbol{\theta}^{(t)}) \quad (6)$$

Here $C^{(t)}$ is an independent constant w.r.t $\boldsymbol{\theta}$, $\mathcal{S}_1(\boldsymbol{\theta}, \boldsymbol{\theta}^{(t)}) = \sum_{n=1}^N \{g_n(\mathbf{w}^{(t)}) + \bar{\mathbf{w}}_t^\top \nabla g_n(\mathbf{w}^{(t)}) + \frac{1}{2} \bar{\mathbf{w}}_t^\top \mathbf{B}_{n,K} \bar{\mathbf{w}}_t\}$, and $\mathcal{S}_2(\boldsymbol{\theta}, \boldsymbol{\theta}^{(t)}) = \sum_{n=1}^N \sum_{k=1}^K \tau_{n,k}^{(t)} \{e_n(\mathbf{c}_k^{(t)}) + \bar{\mathbf{c}}_{k,t}^\top \nabla e_n(\mathbf{c}_k^{(t)}) + \frac{1}{2} \bar{\mathbf{c}}_{k,t}^\top \mathbf{B}_{n,M} \bar{\mathbf{c}}_{k,t}\}$.

These updates in Algorithm 2 minimize the surrogate Equation (6) exactly, and therefore inherit the standard MM monotone-ascent property for the observed-data likelihood via Theorem 2, whose proof follows from the MM majorization–tangency properties of \mathcal{S} and exact minimization; see Section D.3 in the appendix.

Theorem 2 (MM monotonicity for batch SGMLMoE). *Let $\mathcal{S}(\boldsymbol{\theta}, \boldsymbol{\theta}^{(t)})$ be the batch MM surrogate of $-\mathcal{L}(\boldsymbol{\theta})$ in Equation (6) and $\boldsymbol{\theta}^{(t+1)}$ be the output of Algorithm 1. Then, $\boldsymbol{\theta}^{(t+1)} \in \arg \min_{\boldsymbol{\theta}} \mathcal{S}(\boldsymbol{\theta}, \boldsymbol{\theta}^{(t)})$ and $\mathcal{L}(\boldsymbol{\theta}^{(t+1)}) \geq \mathcal{L}(\boldsymbol{\theta}^{(t)})$ for all t .*

4. Fast-rate-aware Aggregation and Sweep-free Model Selection for SGMLMoE

4.1. The “Rate Gap” under Overfitting

In the SGMLMoE classification model Equation (1)–Equation (2), likelihood-based estimation is challenging for the same structural reasons that arise in softmax-gated Gaussian experts (Hai et al., 2026), but with multinomial-logistic experts: (i) *softmax translation invariance* makes gate parameters identifiable only up to a common shift; (ii) *gate–expert coupling* yields nontrivial interactions in local expansions of $s_{\boldsymbol{\theta}}(\cdot | \mathbf{x})$; (iii) *softmax numerator–denominator coupling* creates cancellation phenomena that can make densities close even when individual components are not.

These effects become most visible when the fitted model is *over-specified* ($K > K_0$): several fitted atoms can cluster around a single true expert. In this regime, the conditional density $s_{\widehat{G}_N}(\cdot | \mathbf{x})$ can converge at near-parametric rates in total variation, while componentwise parameters converge more slowly along near-nonidentifiable directions. The goal of this section is to (a) introduce a Voronoi-type loss aligned with the gate-induced partition geometry that resolves these slow directions, and (b) leverage it to build a *hierarchical aggregation path* (a dendrogram of mixing measures) that yields a *sweep-free* and *consistent* selector of the number of experts.

Practical Implication (Single-fit Workflow). Fit one over-specified SGMLMoE (moderate $K \geq K_0$) using the batch MM procedure in Algorithm 2, construct its dendrogram by iterative merging, and select \widehat{K} via a height–likelihood dendrogram selection criterion (DSC). This avoids training multiple models across candidate sizes.

4.2. Mixing-measure Representation for SGMLMoE

Lifted Features and Intercept/Slope Decomposition. With the polynomial degree D fixed, define the non-constant lifted feature map $\phi_D(\mathbf{x}) := \text{vec}([\mathbf{x}^1, \mathbf{x}^2, \dots, \mathbf{x}^D]) \in \mathbb{R}^{PD}$, $\widehat{\mathbf{X}} := \phi_D(\mathbf{X}) \subset \mathbb{R}^{PD}$. (Since \mathbf{X} is compact and ϕ_D is continuous, $\widehat{\mathbf{X}}$ is compact via using Heine-Borel theorem). For each gate $k \in [K-1]$, decompose $w_k(\mathbf{x}) = \bar{w}_k + \hat{w}_k^\top \hat{\mathbf{x}}$, $\hat{\mathbf{x}} := \phi_D(\mathbf{x})$, where $\bar{w}_k := \sum_{p=1}^P w_{k,0,p} \in \mathbb{R}$ and $\hat{w}_k := \text{vec}([\bar{w}_{k,1}, \dots, \bar{w}_{k,D}]) \in \mathbb{R}^{PD}$. For each expert $k \in [K]$ and class $m \in [M-1]$, similarly write $v_{m,k}(\mathbf{x}) = \bar{v}_{m,k} + \hat{v}_{m,k}^\top \hat{\mathbf{x}}$, with $\bar{v}_{m,k} := \sum_{p=1}^P v_{m,k,0,p} \in \mathbb{R}$ and $\hat{v}_{m,k} := \text{vec}([\bar{v}_{m,k,1}, \dots, \bar{v}_{m,k,D}]) \in \mathbb{R}^{PD}$.

Identifiability Conventions (as in Section 2). We fix the reference expert and the reference class: $(\bar{w}_K, \hat{w}_K) = (0, \mathbf{0})$, $(\bar{v}_{M,k}, \hat{v}_{M,k}) = (0, \mathbf{0})$, $\forall k \in [K]$.

Mixing Measures. Let \mathbb{T} denote the identifiable

parameter space for one SGMLMoE atom: $\eta = (\hat{\omega}, \bar{\omega}, \{(\hat{v}_m, \bar{v}_m)\}_{m=1}^{M-1}) \in \mathbb{T}$, and let $\mathcal{O}_K(\mathbb{T})$ be the set of finite mixing measures with at most K atoms: $\mathcal{O}_K(\mathbb{T}) = \{G = \sum_{i=1}^K \pi_i \delta_{\eta_i} : 1 \leq K \leq K, \pi_i > 0, \eta_i \in \mathbb{T}\}$. We parameterize weights by $\pi_i = \exp(\bar{\omega}_i)$ (so $\bar{\omega}_i = \log \pi_i$).

Conditional Probability Mass Function Induced by G . Given $G = \sum_{i=1}^K \pi_i \delta_{\eta_i}$, define for $\hat{x} = \phi_D(\mathbf{x})$ $\mathbf{g}_i(\mathbf{x}; G) = \frac{\pi_i \exp(\hat{\omega}_i^\top \hat{x})}{\sum_{j=1}^K \pi_j \exp(\hat{\omega}_j^\top \hat{x})}$, $\mathbf{e}_i(y = m \mid \mathbf{x}; G) = \frac{\exp(\bar{v}_{m,i} + \hat{v}_{m,i}^\top \hat{x})}{1 + \sum_{\ell=1}^{M-1} \exp(\bar{v}_{\ell,i} + \hat{v}_{\ell,i}^\top \hat{x})}$, with $\mathbf{e}_i(y = M \mid \mathbf{x}; G) = 1 - \sum_{m=1}^{M-1} \mathbf{e}_i(y = m \mid \mathbf{x}; G)$, and $s_G(y \mid \mathbf{x}) = \sum_{i=1}^K \mathbf{g}_i(\mathbf{x}; G) \mathbf{e}_i(y \mid \mathbf{x}; G)$. For any identifiable θ , there exists $G(\theta) \in \mathcal{O}_K(\mathbb{T})$ such that $s_G(\theta) \equiv s_\theta$.

MLE over at most K experts. Let $G_0 \in \mathcal{O}_{K_0}(\mathbb{T})$ be the true mixing measure ($2 \leq K_0 \leq K$). Define the (mixing-measure) MLE $\hat{G}_N \in \arg \max_{G \in \mathcal{O}_K(\mathbb{T})} \frac{1}{N} \sum_{n=1}^N \log s_G(y_n \mid \mathbf{x}_n)$.

4.3. Voronoi Cells and Losses for SGMLMoE

From “Density Closeness” to “Parameter Closeness”. A key step in overfitted mixture/MoE analysis is an *inverse inequality*: small discrepancy between s_G and s_{G_0} should imply small discrepancy between G and G_0 in a geometry-adapted loss. For softmax-gated MoE, the adapted geometry is *Voronoi*: fitted atoms are grouped into cells around each true atom.

Voronoi Partition. Write $G = \sum_{i=1}^K \pi_i \delta_{\eta_i}$ and $G_0 = \sum_{k=1}^{K_0} \pi_k^0 \delta_{\eta_k^0}$. When G is sufficiently close to G_0 (e.g. in the sense below), define a matching $i \mapsto k(i) \in [K_0]$ that assigns each fitted atom η_i to its nearest true atom $\eta_{k(i)}^0$ under the local metric on \mathbb{T} . Define Voronoi cells $\mathbb{V}_k := \{i \in [K] : k(i) = k\}$, $k \in [K_0]$.

Integrated Total Variation Discrepancy. For $\mathbf{x} \in \mathbb{X}$, define $\mathcal{D}_{\text{TV}}(s_G(\cdot \mid \mathbf{x}), s_{G_0}(\cdot \mid \mathbf{x}))$ as $\frac{1}{2} \sum_{m=1}^M |s_G(m \mid \mathbf{x}) - s_{G_0}(m \mid \mathbf{x})|$, and its covariate-averaged version $\mathcal{D}_{\text{TV}}(s_G, s_{G_0})$ as $\mathbb{E}_{\mathbf{x}}[\mathcal{D}_{\text{TV}}(s_G(\cdot \mid \mathbf{x}), s_{G_0}(\cdot \mid \mathbf{x}))]$.

SGMLMoE Voronoi Loss. For $i \in \mathbb{V}_k$, define parameter differences $\Delta\hat{\omega}_{ik} := \hat{\omega}_i - \hat{\omega}_k^0$, $\Delta\bar{v}_{ikm} := \bar{v}_{m,i} - \bar{v}_{m,k}^0$, $\Delta\hat{v}_{ikm} := \hat{v}_{m,i} - \hat{v}_{m,k}^0$, $m \in [M-1]$, and the loss

$$\begin{aligned} \mathcal{D}_{\text{V}}(G, G_0) &= \mathcal{D}_{\text{E}}(G, G_0) \\ &+ \sum_{\substack{k \in [K_0]: |\mathbb{V}_k| > 1 \\ i \in \mathbb{V}_k, m \in [M-1]}} \pi_i [\|\Delta\hat{\omega}_{ik}\|^2 + (|\Delta\bar{v}_{ikm}|^2 + \|\Delta\hat{v}_{ikm}\|^2)], \end{aligned} \quad (7)$$

where $\mathcal{D}_{\text{E}}(G, G_0) := \sum_{k=1}^{K_0} \left| \sum_{i \in \mathbb{V}_k} \pi_i - \pi_k^0 \right| + \sum_{\substack{k \in [K_0]: |\mathbb{V}_k|=1 \\ i \in \mathbb{V}_k, m \in [M-1]}} \pi_i [\|\Delta\hat{\omega}_{ik}\| + (|\Delta\bar{v}_{ikm}| + \|\Delta\hat{v}_{ikm}\|)]$.

Local Structure Inequality (Inverse Bound). The next

result is the “density \Rightarrow Voronoi” inverse bounds developed for SGMLMoE.

Theorem 3. For $G \in \mathcal{O}_K(\mathbb{T})$, as $\mathcal{D}_{\text{TV}}(s_G, s_{G_0}) \rightarrow 0$,

$$\mathcal{D}_{\text{TV}}(s_G, s_{G_0}) \gtrsim \mathcal{D}_{\text{V}}(G, G_0). \quad (8)$$

4.4. Why Merge Experts? The Dendrogram Viewpoint

The Overfitted Picture. When $K > K_0$, some Voronoi cell \mathbb{V}_k may contain multiple fitted atoms. These atoms are “near duplicates” from the perspective of the conditional density, and they create slow/flat directions in the likelihood geometry. The dendrogram mechanism collapses each such cluster by repeated merging, producing a hierarchy of mixing measures $\hat{G}_N^{(K)} = \hat{G}_N \rightsquigarrow \hat{G}_N^{(K-1)} \rightsquigarrow \dots \rightsquigarrow \hat{G}_N^{(2)}$. The key facts we exploit are: (i) each merge reduces redundancy, and (ii) the Voronoi loss becomes easier (monotonically) along the merge chain.

Atom Dissimilarity (Merge Criterion). For two atoms $\pi_i \delta_{\eta_i}$ and $\pi_j \delta_{\eta_j}$, define

$$\begin{aligned} d(\pi_i \delta_{\eta_i}, \pi_j \delta_{\eta_j}) &:= \frac{\pi_i \pi_j}{\pi_i + \pi_j} (\|\hat{\omega}_i - \hat{\omega}_j\|^2 \\ &+ \sum_{m=1}^{M-1} (\|\hat{v}_{m,i} - \hat{v}_{m,j}\|^2 + |\bar{v}_{m,i} - \bar{v}_{m,j}|^2)). \end{aligned} \quad (9)$$

Merge Operator (Weight-averaged Atom). Merging atoms i and j produces a new atom (π_*, η_*) via parameter barycenters for η_* as follows: given any $m \in [M-1]$,

$$\begin{aligned} \pi_* &= \pi_i + \pi_j, \bar{\omega}_* = \log \pi_*, \hat{v}_{m,*} = \frac{\pi_i}{\pi_*} \hat{v}_{m,i} + \frac{\pi_j}{\pi_*} \hat{v}_{m,j}, \\ \bar{v}_{m,*} &= \frac{\pi_i}{\pi_*} \bar{v}_{m,i} + \frac{\pi_j}{\pi_*} \bar{v}_{m,j}, \hat{\omega}_* = \frac{\pi_i}{\pi_*} \hat{\omega}_i + \frac{\pi_j}{\pi_*} \hat{\omega}_j. \end{aligned} \quad (10)$$

Theorem 4 (Voronoi monotonicity along the merge chain). Let $G^{(K)}, G^{(K-1)}, \dots, G^{(K_0)}$ be obtained by repeatedly merging the closest pair of atoms according to Equation (9), starting from $G^{(K)} \in \mathcal{O}_K(\mathbb{T})$. For $G^{(K)}$ sufficiently close to G_0 , $\mathcal{D}_{\text{V}}(G^{(K)}, G_0) \gtrsim \mathcal{D}_{\text{V}}(G^{(K-1)}, G_0) \gtrsim \dots \gtrsim \mathcal{D}_{\text{V}}(G^{(K_0)}, G_0)$.

4.5. Finite-sample Rates along the Dendrogram

Heights (structural signal). At level κ , define the dendrogram height $h_N^{(\kappa)} := \min_{i \neq j \text{ atoms of } \hat{G}_N^{(\kappa)}} d(\pi_i \delta_{\eta_i}, \pi_j \delta_{\eta_j})$, $\kappa \in [K]$, and let $h_0^{(\kappa')}$ be the analogous height on the true chain $G_0^{(\kappa')}, \kappa' \in [K_0]$.

Density Rate for the MLE. We use the known near-parametric bound (up to logs $\tilde{\mathcal{O}}((\log N/N)^{1/2})$) for the MLE in total variation as established for the multinomial classification regime in (Nguyen et al., 2024a):

Fact 1 (Density convergence rate). *There exist universal constants $C_1, C_2 > 0$ such that $\mathbb{P}(\mathcal{D}_{\text{TV}}(s_{\widehat{G}_N}, s_{G_0}) > C_1 \sqrt{\log N/N}) \lesssim N^{-C_2}$.*

From Density Rates to Voronoi and Height Rates. Combining Theorem 3 with Fact 1 yields Voronoi control at level K , and the monotonicity in Theorem 4 propagates it down the path:

Theorem 5 (Voronoi and height rates along the path). *With probability at least $1 - c_1 N^{-c_2}$, for each $\kappa \in \{K_0 + 1, \dots, K\}$ and $\kappa' \in [K_0]$, $\max\{\mathcal{D}_V(\widehat{G}_N^{(\kappa)}, G_0), h_N^{(\kappa)}, |h_N^{(\kappa)} - h_0^{(\kappa')}|\} \lesssim \sqrt{\log N/N}$.*

4.6. Likelihood along the Path and Sweep-free Selection

Empirical and Population Log-likelihoods. For $G \in \mathcal{O}_K(\mathbb{T})$, define $\mathcal{L}(G) := \mathbb{E}_{(\mathbf{x}, \mathbf{y}) \sim G_0} [\log s_G(\mathbf{y} \mid \mathbf{x})]$, and $\bar{\ell}_N(G) := \frac{1}{N} \sum_{n=1}^N \log s_G(y_n \mid \mathbf{x}_n)$. Write $\bar{\ell}_N^{(\kappa)} := \bar{\ell}_N(\widehat{G}_N^{(\kappa)})$.

Condition K (local lower bound). There exist constants $c_\alpha, c_\beta > 0$ such that for all sufficiently small $\epsilon > 0$ and all $\boldsymbol{\theta}, \boldsymbol{\theta}^0 \in \mathbb{T}$ with $\|\boldsymbol{\theta} - \boldsymbol{\theta}^0\| \leq \epsilon$, for all $(\mathbf{x}, \mathbf{y}) \in \mathbb{X} \times \mathbb{Y}$, $\log s_{\boldsymbol{\theta}}(\mathbf{y} \mid \mathbf{x}) \geq (1 + c_\beta \epsilon) \log s_{\boldsymbol{\theta}^0}(\mathbf{y} \mid \mathbf{x}) - c_\alpha \epsilon$.

Theorem 6 (Likelihood control along the dendrogram). *Assume Theorem 5 and Condition K hold. Then, for any $\kappa \in \{K_0 + 1, \dots, K\}$, $\bar{\ell}_N(\widehat{G}_N^{(\kappa)}) - \mathcal{L}(G_0) \lesssim (\log N/N)^{1/4}$. Moreover, for any $\kappa' \in [K_0]$, $\bar{\ell}_N(\widehat{G}_N^{(\kappa')}) \rightarrow \mathcal{L}(G_0^{(\kappa')})$ in \mathbb{P}_{G_0} -probability as $N \rightarrow \infty$.*

DSC (height + likelihood). Given $1 \ll \omega_N \ll (N/\log N)^{1/4}$, define the dendrogram selection criterion $\text{DSC}_N^{(\kappa)} := -\left(h_N^{(\kappa)} + \omega_N \bar{\ell}_N^{(\kappa)}\right)$. A practical choice is $\omega_N = \log N$. Select $\widehat{K}_N := \arg \min_{\kappa \in \{2, \dots, K\}} \text{DSC}_N^{(\kappa)}$.

Theorem 7 (Consistency of DSC for SGMLMoE). *Assume $K_0 \geq 2$ and the conditions of Theorem 6 hold. Then $\widehat{K}_N \rightarrow K_0$ in \mathbb{P}_{G_0} -probability as $N \rightarrow \infty$.*

Interpretation of Why DSC Beats Pure Likelihood Penalties under Overfit. Heights detect structural redundancy: small $h_N^{(\kappa)}$ indicates that the κ -atom model contains a pair of nearly indistinguishable atoms (often created by over-specification), which standard criteria (AIC/BIC/ICL) do not directly penalize. DSC combines this structural signal with fit, yielding a sweep-free selector aligned with the Voronoi geometry.

5. Numerical Experiment

In this section, we conduct experiments on both synthetic and real-world datasets to systematically evaluate the effectiveness, stability, and practical utility of the proposed

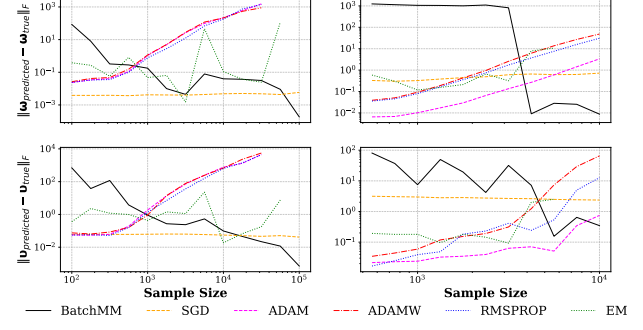


Figure 2. Convergence behavior of the Batch MM algorithm (parameter error versus sample size).

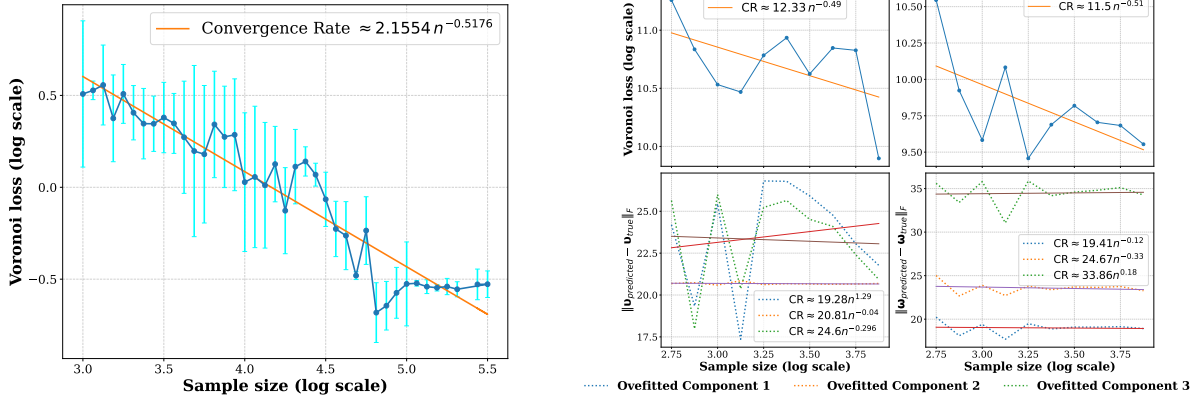
pipeline: batch MM training, Voronoi-loss diagnostics, and dendrogram-based selection/merging via DSC. On *synthetic datasets*, we first demonstrate that the proposed Batch MM algorithm converges reliably to the global optimum, while classical optimization methods, including EM and popular gradient-based optimizers, often become trapped at sub-optimal stationary points, in both well-specified and over-parameterized regimes. We then empirically verify that the decay of the Voronoi loss aligns with the finite-sample convergence rates established in Theorem 5, under both exact-fit and over-fit settings. Finally, we show that the proposed DSC-based merging strategy consistently outperforms standard model selection criteria (AIC, BIC, and ICL) in recovering the true number of experts, especially in small-sample regimes, while retaining consistency as sample size grows. On *real-world datasets*, we show that SGMLMoE trained via Batch MM yields superior predictive performance compared to strong baselines such as SVM and Random Forest. Moreover, DSC selects an appropriate number of experts that achieves an attractive trade-off between predictive accuracy and memory efficiency, while the resulting dendrogram provides an interpretable hierarchical summary of the fitted mixing measure via Figure 5.

5.1. Simulation Study

Dataset. We consider a controlled synthetic setting with polynomial degree $D = 1$, number of experts $K_0 = 2$, number of categories $M = 2$, and input dimension $P = 1$. The ground-truth gate parameters are $\omega_{0,0,0} = \omega_{1,0,0} = \omega_{1,1,0} = 0$ and $\omega_{0,0,1} = 8$, and the expert parameters are $\mathbf{v}_{0,0,0,0} = \mathbf{v}_{1,0,1,0} = \mathbf{v}_{0,1,0,0} = \mathbf{v}_{1,1,1,0} = 0$, $\mathbf{v}_{0,0,1,0} = \mathbf{v}_{0,1,1,0} = 20$, and $\mathbf{v}_{1,0,0,0} = -\mathbf{v}_{1,1,0,0} = 10$. To generate the dataset (\mathbb{X}, \mathbb{Y}) , we first fix a sample size N (which varies across experiments). We then sample inputs $\mathbb{X} = \{\mathbf{x}_n\}_{n=1}^N$ i.i.d. from the standard normal distribution $\mathcal{N}(0, 1)$. Conditional on \mathbb{X} , we generate discrete outputs $\mathbb{Y} = \{y_n\}_{n=1}^N$ according to the SGMLMoE model specified by (ω_0, \mathbf{v}_0) .

Table 1. Summary of (log-adjusted) density and parameter rates for SGMLMoE with standard softmax gating.

Setting	Density	Exact-specified Parameters ($ \mathbb{V}_k = 1$)	Over-specified Parameters ($ \mathbb{V}_k > 1$)
Exact-fit	$\tilde{\mathcal{O}}((\log N/N)^{1/2})$	$\tilde{\mathcal{O}}((\log N/N)^{1/2})$	—
Over-fit	$\tilde{\mathcal{O}}((\log N/N)^{1/2})$	$\tilde{\mathcal{O}}((\log N/N)^{1/2})$	$\tilde{\mathcal{O}}((\log N/N)^{1/4})$
Merged	$\tilde{\mathcal{O}}((\log N/N)^{1/2})$	$\tilde{\mathcal{O}}((\log N/N)^{1/2})$	$\tilde{\mathcal{O}}((\log N/N)^{1/2})$



(a) Exact-fit: empirical convergence of the Voronoi loss.

Figure 3. Empirical convergence of the Voronoi loss under exact specification and over-specification.

Initialization. In the well-specified setting ($K = K_0$), parameters are initialized by perturbing the ground-truth values ω_0 and v_0 with additive Gaussian noise: each coordinate is set to the corresponding ground-truth value plus an independent $\mathcal{N}(0, 1)$ perturbation, scaled by a prescribed noise level. In the over-parameterized setting ($K > K_0$), we introduce additional expert components beyond the truth. For each extra cluster $k \in \{K_0 + 1, \dots, K\}$, we set $\omega_{k,0,0} = 0$, $\omega_{k,0,1} = 8$, $v_{0,k,0,0} = v_{1,k,1,0} = 0$, $v_{0,k,1,0} = 20$, and $v_{1,k,0,0} = 10$. The original K_0 experts are initialized as in the well-specified case. This design ensures that over-parameterization genuinely creates near-duplicate atoms, which is precisely the regime targeted by our Voronoi analysis and merging strategy.

Convergence of BatchMM. We study the convergence behavior of SGMLMoE trained using the proposed Batch MM algorithm, and compare it against classical optimization methods, including stochastic gradient descent (SGD), Adam, AdamW, RMSprop, and EM. In the well-specified setting, we vary the sample size from $N = 10^2$ to $N = 10^5$. In the over-parameterized setting, we fix $K = 3$ and vary N from $10^{2.75}$ to 10^4 . Convergence is evaluated via the Frobenius norm between the estimated parameters (ω, v) and the ground-truth (ω_0, v_0). As shown in Figure 2, Batch MM consistently converges to the global minimum, while the competing methods are often markedly slower and, in the over-parameterized regime, frequently converge to sub-optimal solutions as N grows.

Convergence of Voronoi Loss. We empirically verify the

convergence rates predicted by Theorem 5. In the exact-fit setting (Figure 3a), varying the sample size from 10^3 to $10^{5.5}$ yields a log-log slope consistent with the parametric rate $N^{-1/2}$. In the over-specified setting with $K \in \{3, 4\}$ and $N \in [10^{2.5}, 10^4]$, the fitted regression lines in Figure 3b match the predicted rates. For $K = 4$, the Frobenius error of individual components shows that one spurious component converges at a slower sub-parametric rate, empirically close to $N^{-0.25}$, in agreement with the rate predicted by Theorem 5 for over-covered Voronoi cells. In contrast, another overfitted component exhibits increasing error as N grows, reflecting a mild repulsion effect in over-parameterized models whereby redundant components are displaced away from the true parameters to resolve non-identifiability (here the relevant cells are \mathbb{V}_k).

Merging using DSC. Finally, we evaluate the effectiveness of our DSC-based merging strategy for recovering the correct number of experts. We fix $K = 4$ and vary the sample size from $N = 10^2$ to 10^4 . For each N , we repeat the experiment 20 times with different random seeds. We compare DSC against AIC, BIC, and ICL by recording (i) the frequency with which each criterion selects the correct number of experts and (ii) the average number of selected experts; results are shown in Figure 4. Across sample sizes, DSC exhibits a higher correct-selection frequency than the baseline criteria. In particular, in the small-sample regime, DSC is notably more robust, while for sufficiently large N it consistently recovers the true number of experts, matching the consistency guarantees established in our theory.

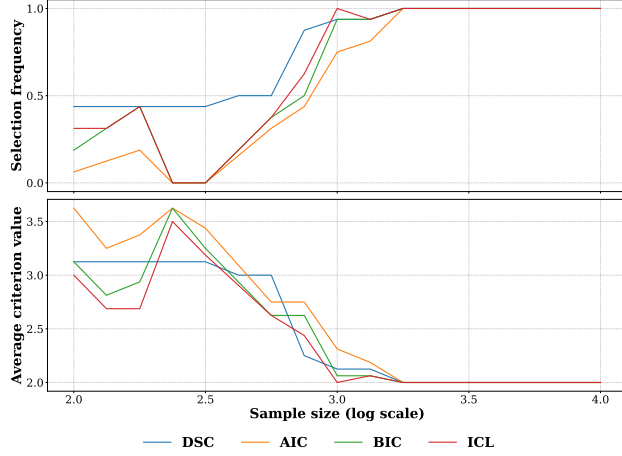


Figure 4. DSC model selection performance.

5.2. Real Dataset

Initialization. Since the true latent expert assignments are unknown in real data, we adopt a practical two-stage initialization strategy grounded in unsupervised learning. We first apply a classical clustering method (e.g., K-means or spectral clustering) to obtain preliminary groupings. We then construct initial SGMLMoE parameters from these assignments, providing a structured, data-informed initialization for Batch MM.

Expert Estimation. We use a subset of 5,000 samples from a protein–protein interaction prediction dataset (Tang et al., 2023b; Qi et al., 2007) to train the proposed DSC method as well as baseline criteria including AIC, BIC, and ICL for selecting the number of experts, with the maximum capped at $K = 8$. A separate set of 5,000 samples is then used for model training and cross-validation across candidate values of K . Table 2 reports cross-validation performance as a function of K , along with the expert count selected by each criterion. DSC selects $K = 3$, achieving strong predictive performance while maintaining a compact model. In contrast, ICL favors a smaller model ($K = 2$), leading to reduced precision and F1 score, whereas AIC and BIC select larger models ($K = 4$), increasing complexity with only marginal performance gains. Overall, these results show that DSC achieves a better trade-off between accuracy and model complexity than classical criteria.

Accuracy Comparison. We fix the number of experts to $K = 3$ and train SGMLMoE using the Batch MM algorithm on 5,000 samples. We compare its performance with standard baseline methods, Naive Bayes, Random Forest, Support Vector Machine, and Logistic Regression, using recall, precision, and F1 score. As shown in Table 3, SGMLMoE achieves the best overall performance among all methods, attaining the highest precision (0.74) and F1 score (0.80), while maintaining competitive recall (0.88). Naive Bayes

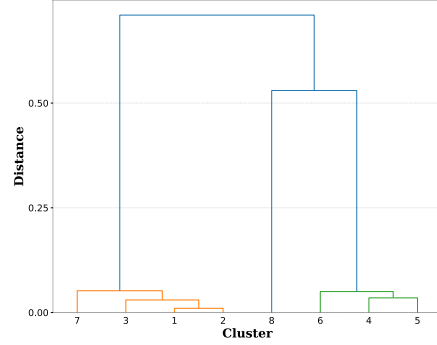


Figure 5. Dendrogram of mixing measure.

K	Recall	Precision	F1	# P	CoMs
1	0.54 ± 0.04	0.43 ± 0.03	0.48 ± 0.003	6	
2	0.72 ± 0.02	0.61 ± 0.02	0.66 ± 0.003	12	ICL
3	0.88 ± 0.01	0.73 ± 0.02	0.80 ± 0.003	18	DSC
4	0.88 ± 0.01	0.74 ± 0.01	0.80 ± 0.002	24	AIC, BIC
5	0.89 ± 0.01	0.75 ± 0.01	0.81 ± 0.002	30	
6	0.91 ± 0.01	0.76 ± 0.01	0.83 ± 0.001	36	
7	0.92 ± 0.01	0.76 ± 0.01	0.83 ± 0.001	42	
8	0.92 ± 0.01	0.76 ± 0.01	0.83 ± 0.001	48	

 Table 2. Performance across number of experts K .

exhibits lower precision and F1 score, indicating limited discriminative capacity, while Random Forest, SVM, Logistic Regression, and 3-Hidden Layer MLP improve upon NB but remain consistently below SGMLMoE in precision and overall F1. These results underscore the benefit of SGMLMoE in capturing heterogeneity, and they empirically support the practical stability of Batch MM relative to standard training baselines. Finally, Figure 5 displays the dendrogram of the fitted mixing measure obtained by Algorithm 2, which provides an interpretable hierarchical view of the inferred expert structure.

Conclusion and Perspectives. In summary, our experiments confirm the paper’s main message: Batch MM yields stable maximum-likelihood training for SGMLMoE in the full-data regime, while the Voronoi-loss/dendrogram view provides a principled remedy for over-parameterization. Em-

Table 3. Comparison with baseline methods.

Method	Recall	Precision	F1
SGMLMoE	0.88 ± 0.012	0.74 ± 0.010	0.80 ± 0.002
NB	0.83 ± 0.011	0.64 ± 0.009	0.72 ± 0.001
RF	0.85 ± 0.012	0.68 ± 0.008	0.76 ± 0.001
SVM	0.85 ± 0.010	0.69 ± 0.009	0.76 ± 0.002
LR	0.84 ± 0.014	0.65 ± 0.009	0.73 ± 0.003
3HL-MLP	0.87 ± 0.008	0.71 ± 0.009	0.77 ± 0.001

pirically, Batch MM converges reliably, the Voronoi loss decays in line with the predicted finite-sample rates, and DSC consistently selects a compact expert count that preserves accuracy and improves calibration on protein–protein interaction prediction. Future work includes extending the MM surrogates to incremental/mini-batch settings, broadening the dendrogram theory to richer expert parameterizations and structured regularization, and developing robustness guarantees under contamination and covariate shift.

Impact Statement

This paper presents work whose goal is to advance the field of Machine Learning. There are many potential societal consequences of our work, none which we feel must be specifically highlighted here

References

Akaike, H. A new look at the statistical model identification. *IEEE Transactions on Automatic Control*, 19(6):716–723, 1974.

Bengio, Y. Deep Learning of Representations: Looking Forward. In *Statistical Language and Speech Processing*, pp. 1–37, Berlin, Heidelberg, 2013. ISBN 978-3-642-39593-2.

Berrettini, M., Galimberti, G., Ranciati, S., and Murphy, T. B. Identifying Brexit voting patterns in the British house of commons: an analysis based on Bayesian mixture models with flexible concomitant covariate effects. *Journal of the Royal Statistical Society Series C: Applied Statistics*, 73(3):621–638, June 2024. ISSN 0035-9254.

Biernacki, C., Celeux, G., and Govaert, G. Assessing a mixture model for clustering with the integrated completed likelihood. *IEEE Transactions on Pattern Analysis and Machine Intelligence*, 22(7):719–725, 2000.

Borkar, V. S. *Stochastic approximation: a dynamical systems viewpoint*, volume 9. Springer, 2008.

Cai, W., Jiang, J., Wang, F., Tang, J., Kim, S., and Huang, J. A Survey on Mixture of Experts in Large Language Models. *IEEE Transactions on Knowledge and Data Engineering*, 37(7):3896–3915, 2025.

Cappé, O. Online EM Algorithm for Hidden Markov Models. *Journal of Computational and Graphical Statistics*, 20(3):728–749, January 2011. ISSN 1061-8600.

Cappé, O. and Moulines, E. On-Line Expectation–Maximization Algorithm for latent Data Models. *Journal of the Royal Statistical Society Series B: Statistical Methodology*, 71(3):593–613, February 2009. ISSN 1369-7412.

Chen, J., Zhu, J., Teh, Y. W., and Zhang, T. Stochastic Expectation Maximization with Variance Reduction. In Bengio, S., Wallach, H., Larochelle, H., Grauman, K., Cesa-Bianchi, N., and Garnett, R. (eds.), *Advances in Neural Information Processing Systems*, volume 31. Curran Associates, Inc., 2018.

Chen, K., Xu, L., and Chi, H. Improved learning algorithms for mixture of experts in multiclass classification. *Neural Networks*, 12(9):1229–1252, 1999. ISSN 0893-6080.

Chen, Z., Deng, Y., Wu, Y., Gu, Q., and Li, Y. Towards Understanding the Mixture-of-Experts Layer in Deep Learning. In *Advances in Neural Information Processing Systems*, 2022.

Chong, M. C., Nguyen, H. D., and Nguyen, T. Risk Bounds for Mixture Density Estimation on Compact Domains via the h -Lifted Kullback–Leibler Divergence. *Transactions on Machine Learning Research*, 2024. ISSN 2835-8856.

Consortium, U. Uniprot: a hub for protein information. *Nucleic acids research*, 43(D1):D204–D212, 2015.

Corff, S. L. and Fort, G. Online Expectation Maximization based algorithms for inference in Hidden Markov Models. *Electronic Journal of Statistics*, 7(none):763 – 792, 2013.

De Leeuw, J. Application of convex analysis to multidimensional scaling. *Recent developments in statistics*, pp. 133–145, 1977.

De Leeuw, J. and Heiser, W. J. Convergence of correction matrix algorithms for multidimensional scaling. *Geometric representations of relational data*, 36:735–752, 1977.

Dempster, A. P., Laird, N. M., and Rubin, D. B. Maximum Likelihood from Incomplete Data via the EM Algorithm. *Journal of the Royal Statistical Society. Series B (Methodological)*, 39(1):1–38, mar 1977. ISSN 00359246.

Dieuleveut, A., Fort, G., Moulines, E., and Wai, H.-T. Stochastic Approximation Beyond Gradient for Signal Processing and Machine Learning. *IEEE Transactions on Signal Processing*, 71:3117–3148, 2023.

Do, D., Do, L., McKinley, S. A., Terhorst, J., and Nguyen, X. Dendrogram of mixing measures: Learning latent hierarchy and model selection for finite mixture models. *arXiv preprint arXiv:2403.01684*, 2024.

Do, D., Do, L., and Nguyen, X. Strong identifiability and parameter learning in regression with heterogeneous response. *Electronic Journal of Statistics*, 19(1):131 – 203, 2025.

Forbes, F., Nguyen, H. D., Nguyen, T., and Arbel, J. Mixture of expert posterior surrogates for approximate Bayesian computation. In *JDS 2022 - 53èmes Journées de Statistique de la Société Française de Statistique (SFdS)*, Lyon, France, June 2022a.

Forbes, F., Nguyen, H. D., Nguyen, T., and Arbel, J. Summary statistics and discrepancy measures for approximate Bayesian computation via surrogate posteriors. *Statistics and Computing*, 32(5):85, October 2022b. ISSN 1573-1375.

Fort, G. and Moulines, E. The Perturbed Prox-Preconditioned Spider Algorithm: Non-Asymptotic Convergence Bounds. In *2021 IEEE Statistical Signal Processing Workshop (SSP)*, pp. 96–100, 2021.

Fort, G. and Moulines, E. Stochastic variable metric proximal gradient with variance reduction for non-convex composite optimization. *Statistics and Computing*, 33(3), April 2023. ISSN 1573-1375.

Fort, G., Moulines, E., and Wai, H.-T. A Stochastic Path Integral Differential EstimatoR Expectation Maximization Algorithm. In Larochelle, H., Ranzato, M., Hadsell, R., Balcan, M. F., and Lin, H. (eds.), *Advances in Neural Information Processing Systems*, volume 33, pp. 16972–16982. Curran Associates, Inc., 2020.

Fort, G., Gach, P., and Moulines, E. Fast incremental expectation maximization for finite-sum optimization: nonasymptotic convergence. *Statistics and Computing*, 31(4):48, June 2021a. ISSN 1573-1375.

Fort, G., Moulines, E., and Wai, H.-T. Geom-Spider-EM: Faster Variance Reduced Stochastic Expectation Maximization for Nonconvex Finite-Sum Optimization. In *ICASSP 2021 - 2021 IEEE International Conference on Acoustics, Speech and Signal Processing (ICASSP)*, pp. 3135–3139, 2021b.

Foygel, R. and Drton, M. Extended Bayesian Information Criteria for Gaussian Graphical Models. In Lafferty, J., Williams, C., Shawe-Taylor, J., Zemel, R., and Culotta, A. (eds.), *Advances in Neural Information Processing Systems*, volume 23. Curran Associates, Inc., 2010.

Frühwirth-Schnatter, S. Keeping the balance—Bridge sampling for marginal likelihood estimation in finite mixture, mixture of experts and Markov mixture models. *Brazilian Journal of Probability and Statistics*, 33(4):706 – 733, 2019.

Frühwirth-Schnatter, S., Pamminger, C., Weber, A., and Winter-Ebmer, R. Labor market entry and earnings dynamics: Bayesian inference using mixtures-of-experts Markov chain clustering. *Journal of Applied Econometrics*, 27(7):1116–1137, 2012.

Frühwirth-Schnatter, S., Pittner, S., Weber, A., and Winter-Ebmer, R. Analysing plant closure effects using time-varying mixture-of-experts Markov chain clustering. *The Annals of Applied Statistics*, 12(3):1796 – 1830, 2018. Publisher: Institute of Mathematical Statistics.

Genovese, C. R. and Wasserman, L. Rates of convergence for the Gaussian mixture sieve. *The Annals of Statistics*, 28(4):1105 – 1127, 2000.

Guha, A., Ho, N., and Nguyen, X. On posterior contraction of parameters and interpretability in Bayesian mixture modeling. *Bernoulli*, 27(4):2159 – 2188, 2021.

Hai, D. T., Mai, T. N., Nguyen, T., Ho, N., Nguyen, B. T., and Drovandi, C. Dendrograms of Mixing Measures for Softmax-Gated Gaussian Mixture of Experts: Consistency without Model Sweeps. In *Proceedings of The 29th International Conference on Artificial Intelligence and Statistics*, Proceedings of Machine Learning Research. PMLR, 2026.

Hennig, C. Identifiability of Models for Clusterwise Linear Regression. *Journal of Classification*, 17(2):273–296, 2000. ISSN 1432-1343.

Ho, B. H., Chi, L. N., Nguyen, T., Hoang, V. H., Nguyen, B. T., and Drovandi, C. A Unified Framework for Variable Selection in Model-Based Clustering with Missing Not at Random. In *The Thirty-ninth Annual Conference on Neural Information Processing Systems*, 2025.

Ho, N. and Nguyen, X. Convergence rates of parameter estimation for some weakly identifiable finite mixtures. *The Annals of Statistics*, 44(6):2726 – 2755, 2016a.

Ho, N. and Nguyen, X. On strong identifiability and convergence rates of parameter estimation in finite mixtures. *Electronic Journal of Statistics*, 10(1):271–307, 2016b.

Ho, N. and Nguyen, X. Singularity Structures and Impacts on Parameter Estimation in Finite Mixtures of Distributions. *SIAM Journal on Mathematics of Data Science*, 1 (4):730–758, jan 2019.

Ho, N., Yang, C.-Y., and Jordan, M. I. Convergence Rates for Gaussian Mixtures of Experts. *Journal of Machine Learning Research*, 2022.

Huynh, B. T. and Chamroukhi, F. Estimation and feature selection in mixtures of generalized linear experts models. *arXiv preprint arXiv:1907.06994*, 2019.

Jacobs, R. A., Jordan, M. I., Nowlan, S. J., and Hinton, G. E. Adaptive mixtures of local experts. *Neural computation*, 3(1):79–87, 1991. Publisher: MIT Press.

Jiang, W. and Tanner, M. A. On the identifiability of mixtures-of-experts. *Neural Networks*, 12(9):1253–1258, 1999a. ISSN 0893-6080.

Jiang, W. and Tanner, M. A. Hierarchical mixtures-of-experts for exponential family regression models: approximation and maximum likelihood estimation. *Annals of Statistics*, pp. 987–1011, 1999b.

Jordan, M. I. and Jacobs, R. A. Hierarchical mixtures of experts and the EM algorithm. *Neural computation*, 6(2): 181–214, 1994. Publisher: MIT Press.

Karimi, B., Miasojedow, B., Moulines, E., and Wai, H.-T. Non-asymptotic Analysis of Biased Stochastic Approximation Scheme. In Beygelzimer, A. and Hsu, D. (eds.), *Proceedings of the Thirty-Second Conference on Learning Theory*, volume 99 of *Proceedings of Machine Learning Research*, pp. 1944–1974. PMLR, June 2019a.

Karimi, B., Wai, H.-T., Moulines, E., and Lavielle, M. On the Global Convergence of (Fast) Incremental Expectation Maximization Methods. In *Advances in Neural Information Processing Systems*, volume 32, 2019b.

Keener, R. W. *Theoretical statistics: Topics for a core course*. Springer Science & Business Media, 2010.

Khalili, A., Yang, A. Y., and Da, X. Estimation and group-feature selection in sparse mixture-of-experts with diverging number of parameters. *Journal of Statistical Planning and Inference*, pp. 106250, 2024. ISSN 0378-3758.

Kuhn, E., Matias, C., and Rebafka, T. Properties of the stochastic approximation EM algorithm with mini-batch sampling. *Statistics and Computing*, 30(6):1725–1739, November 2020. ISSN 1573-1375.

Kushner, H. and Yin, G. G. *Stochastic Approximation and Recursive Algorithms and Applications*, volume 35. Springer Science & Business Media, 2003.

Lange, K. *MM Optimization Algorithms*. Society for Industrial and Applied Mathematics, Philadelphia, PA, 2016.

Lange, K., Won, J.-H., Landeros, A., and Zhou, H. Non-convex Optimization via MM Algorithms: Convergence Theory. In *Wiley StatsRef: Statistics Reference Online*, pp. 1–22. John Wiley & Sons, Ltd, 2021. ISBN 978-1-118-44511-2.

Mairal, J. Stochastic majorization-minimization algorithms for large-scale optimization. *Advances in Neural Information Processing Systems*, 26, 2013.

Mairal, J. Incremental Majorization-Minimization Optimization with Application to Large-Scale Machine Learning. *SIAM Journal on Optimization*, 25(2):829–855, 2015.

Masoudnia, S. and Ebrahimpour, R. Mixture of experts: a literature survey. *Artificial Intelligence Review*, 42(2): 275–293, 2014. ISSN 1573-7462.

McLachlan, G. J. and Krishnan, T. *The EM Algorithm and Extensions*. Wiley, 1997.

Meilijson, I. A Fast Improvement to the Em Algorithm on its Own Terms. *Journal of the Royal Statistical Society: Series B (Methodological)*, 51(1):127–138, September 1989. ISSN 0035-9246.

Montuelle, L. and Le Pennec, E. Mixture of Gaussian regressions model with logistic weights, a penalized maximum likelihood approach. *Electronic Journal of Statistics*, 8(1):1661–1695, 2014.

Neal, R. M. and Hinton, G. E. A View of the EM Algorithm that Justifies Incremental, Sparse, and other Variants. In Jordan, M. I. (ed.), *Learning in Graphical Models*, pp. 355–368. Springer Netherlands, Dordrecht, 1998. ISBN 978-94-011-5014-9.

Nguyen, D. N. and Li, Z. Joint learning of Gaussian graphical models in heterogeneous dependencies of high-dimensional transcriptomic data. In *The 16th Asian Conference on Machine Learning (Conference Track)*, 2024.

Nguyen, H., Nguyen, T., and Ho, N. Demystifying Softmax Gating in Gaussian Mixture of Experts. In *Advances in Neural Information Processing Systems*, December 2023a.

Nguyen, H., Akbarian, P., Nguyen, T., and Ho, N. A General Theory for Softmax Gating Multinomial Logistic Mixture of Experts. In *Proceedings of The 41st International Conference on Machine Learning*, 2024a.

Nguyen, H., Nguyen, T., Nguyen, K., and Ho, N. Towards Convergence Rates for Parameter Estimation in Gaussian-gated Mixture of Experts. In *Proceedings of The 27th International Conference on Artificial Intelligence and Statistics*, volume 238, pp. 2683–2691, May 2024b.

Nguyen, H. D. An introduction to Majorization-Minimization algorithms for machine learning and statistical estimation. *WIREs Data Mining and Knowledge Discovery*, 7(2):e1198, 2017.

Nguyen, H. D. and Chamroukhi, F. Practical and theoretical aspects of mixture-of-experts modeling: An overview. *Wiley Interdisciplinary Reviews: Data Mining and Knowledge Discovery*, 8(4):e1246, 2018.

Nguyen, H. D. and Nguyen, T. Modifications of the BIC for order selection in finite mixture models. 2506.20124, 2025.

Nguyen, H. D., Lloyd-Jones, L. R., and McLachlan, G. J. A universal approximation theorem for mixture-of-experts models. *Neural computation*, 28(12):2585–2593, 2016. Publisher: MIT Press.

Nguyen, H. D., Chamroukhi, F., and Forbes, F. Approximation results regarding the multiple-output Gaussian gated mixture of linear experts model. *Neurocomputing*, 366:208–214, 2019. ISSN 0925-2312.

Nguyen, H. D., Forbes, F., and McLachlan, G. J. Mini-batch learning of exponential family finite mixture models. *Statistics and Computing*, 30(4):731–748, July 2020a. ISSN 1573-1375.

Nguyen, H. D., Nguyen, T., Chamroukhi, F., and McLachlan, G. J. Approximations of conditional probability density functions in Lebesgue spaces via mixture of experts models. *Journal of Statistical Distributions and Applications*, 8(1):13, August 2021a. ISSN 2195-5832.

Nguyen, H. D., Nguyen, T., and Forbes, F. Bayesian Likelihood Free Inference using Mixtures of Experts. In *2024 International Joint Conference on Neural Networks (IJCNN)*, pp. 1–8, 2024c.

Nguyen, T. *Model Selection and Approximation in High-dimensional Mixtures of Experts Models: from Theory to Practice*. PhD Thesis, Normandie Université, December 2021.

Nguyen, T., Nguyen, H. D., Chamroukhi, F., and McLachlan, G. J. Approximation by finite mixtures of continuous density functions that vanish at infinity. *Cogent Mathematics & Statistics*, 7(1):1750861, 2020b.

Nguyen, T., Chamroukhi, F., Nguyen, H. D., and Forbes, F. Non-asymptotic model selection in block-diagonal mixture of polynomial experts models. *Preprint. arXiv:2104.08959*, May 2021b.

Nguyen, T., Chamroukhi, F., Nguyen, H. D., and Forbes, F. Model selection by penalization in mixture of experts models with a non-asymptotic approach. In *JDS 2022 - 53èmes Journées de Statistique de la Société Française de Statistique (SFdS)*, Lyon, France, June 2022a.

Nguyen, T., Chamroukhi, F., Nguyen, H. D., and McLachlan, G. J. Approximation of probability density functions via location-scale finite mixtures in Lebesgue spaces. *Communications in Statistics - Theory and Methods*, pp. 1–12, May 2022b. ISSN 0361-0926.

Nguyen, T., Nguyen, H. D., Chamroukhi, F., and Forbes, F. A non-asymptotic approach for model selection via penalization in high-dimensional mixture of experts models. *Electronic Journal of Statistics*, 16(2):4742 – 4822, 2022c.

Nguyen, T., Nguyen, D. N., Nguyen, H. D., and Chamroukhi, F. A non-asymptotic theory for model selection in high-dimensional mixture of experts via joint rank and variable selection. In *AJCAI Australasian Joint Conference on Artificial Intelligence 2023*, December 2023b.

Nguyen, T., Nguyen, H. D., Chamroukhi, F., and McLachlan, G. J. Non-asymptotic oracle inequalities for the Lasso in high-dimensional mixture of experts. *arXiv:2009.10622*, February 2023c.

Nguyen, T., Forbes, F., Arbel, J., and Duy Nguyen, H. Bayesian nonparametric mixture of experts for inverse problems. *Journal of Nonparametric Statistics*, pp. 1–60, May 2024d. ISSN 1048-5252.

Nguyen, X. Convergence of latent mixing measures in finite and infinite mixture models. *The Annals of Statistics*, 41(1):370–400, 2013.

Norets, A. Approximation of conditional densities by smooth mixtures of regressions. *The Annals of Statistics*, 38(3):1733 – 1766, 2010.

Ortega, J. and Rheinboldt, W. *Iterative Solution of Nonlinear Equations in Several Variables*, volume 30. SIAM, 1970.

Oudoumanessah, G., Coudert, T., Lartizien, C., Dojat, M., Christen, T., and Forbes, F. Scalable magnetic resonance fingerprinting: Incremental inference of high dimensional elliptical mixtures from large data volumes, 2024.

Oudoumanessah, G., Coudert, T., Meyer, L., Delphin, A., Dojat, M., Lartizien, C., and Forbes, F. Cluster globally, reduce locally: Scalable efficient dictionary compression for magnetic resonance fingerprinting. In *IEEE International Symposium on Biological Imaging (ISBI)*, 2025.

Pham, N. T. and Chamroukhi, F. Functional mixture-of-experts for classification. In *53èmes Journées de Statistique de la Société Française de Statistique (SFdS)*, 2022.

Qi, Y., Klein-Seetharaman, J., and Bar-Joseph, Z. A mixture of feature experts approach for protein-protein interaction prediction. *BMC Bioinformatics*, 8(10):S6, December 2007. ISSN 1471-2105.

Rakhlin, A., Panchenko, D., and Mukherjee, S. Risk bounds for mixture density estimation. *ESAIM: PS*, 9:220–229, 2005.

Schwarz, G. Estimating the dimension of a model. *The Annals of Statistics*, 6(2):461–464, 1978.

Sin, C.-Y. and White, H. Information criteria for selecting possibly misspecified parametric models. *Journal of Econometrics*, 71(1):207–225, 1996. ISSN 0304-4076.

Sun, Y., Babu, P., and Palomar, D. P. Majorization-Minimization Algorithms in Signal Processing, Communications, and Machine Learning. *IEEE Transactions on Signal Processing*, 65(3):794–816, 2017.

Tang, T., Zhang, X., Liu, Y., Peng, H., Zheng, B., Yin, Y., and Zeng, X. Machine learning on protein–protein interaction prediction: models, challenges and trends. *Briefings in Bioinformatics*, 24(2):bbad076, 2023a.

Tang, T., Zhang, X., Liu, Y., Peng, H., Zheng, B., Yin, Y., and Zeng, X. Machine learning on protein–protein interaction prediction: models, challenges and trends. *Briefings in Bioinformatics*, 24(2):bbad076, March 2023b. ISSN 1477-4054.

Thai, T., Nguyen, T., Do, D., Ho, N., and Drovandi, C. Model Selection for Gaussian-gated Gaussian Mixture of Experts Using Dendrograms of Mixing Measures. *arXiv preprint arXiv:2505.13052*, 2025.

Van de Geer, S. *Empirical Processes in M-estimation*, volume 6. Cambridge university press, 2000.

Wang, Z., Ji, K., Zhou, Y., Liang, Y., and Tarokh, V. SpiderBoost and Momentum: Faster Variance Reduction Algorithms. In Wallach, H., Larochelle, H., Beygelzimer, A., Alché-Buc, F. d., Fox, E., and Garnett, R. (eds.), *Advances in Neural Information Processing Systems*, volume 32. Curran Associates, Inc., 2019.

Westerhout, J., Nguyen, T., Guo, X., and Nguyen, H. D. On the Asymptotic Distribution of the Minimum Empirical Risk. In *Forty-first International Conference on Machine Learning*, 2024.

Yuksel, S. E. and Gader, P. Variational Mixture of Experts for Classification with Applications to Landmine Detection. In *2010 20th International Conference on Pattern Recognition*, pp. 2981–2984, 2010.

Yuksel, S. E., Wilson, J. N., and Gader, P. D. Twenty Years of Mixture of Experts. *IEEE Transactions on Neural Networks and Learning Systems*, 23(8):1177–1193, 2012. ISSN 2162-2388 VO - 23.

Zens, G. Bayesian shrinkage in mixture-of-experts models: identifying robust determinants of class membership. *Advances in Data Analysis and Classification*, 13(4):1019–1051, December 2019. ISSN 1862-5355.

Supplementary Materials for “Fast Model Selection and Stable Optimization for Softmax-Gated Multinomial-Logistic Mixture of Experts Models”

Appendix Organization. This appendix collects material that supports the main paper at three complementary levels. [Section A](#) extends the discussion with empirical takeaways and concrete future directions. [Section B](#) provides implementation-ready details of the Batch MM routine for SGMLMoE, including the linear-algebra identities, the full algorithmic steps, and practical notes on conditioning and stopping. [Section C](#) documents experimental protocols (data preprocessing, evaluation, and reproducibility details). Finally, [Section D](#) contains complete proofs.

A. Extended Conclusion and Perspectives

Overall, the numerical experiments support the main message of the paper: in SGMLMoE, the proposed Batch MM updates provide a stable and reliable maximum-likelihood training routine in the full-data regime, and the Voronoi-loss/dendrogram viewpoint yields a practically effective handle on over-parameterization. Empirically, we observe (i) monotone and repeatable likelihood improvement with Batch MM across well-specified and over-specified settings, (ii) decay of the Voronoi loss consistent with the finite-sample theory in both exact-fit and over-fit regimes, and (iii) robust recovery of the effective number of experts via DSC, which translates into compact models with competitive or improved predictive performance and probability calibration on protein–protein interaction data.

Looking forward, several extensions are natural. First, it would be valuable to couple the present batch-MM stability guarantees with incremental or mini-batch variants to handle larger-scale datasets while preserving the monotone-surrogate structure. Second, extending the dendrogram/DSC analysis to richer expert parameterizations (e.g., deeper feature maps, structured sparsity, or context-dependent expert sharing) could broaden applicability while maintaining interpretability through the merging hierarchy. Third, the robustness observed under mild misspecification suggests studying contamination and covariate-shift regimes theoretically, with DSC-style structural penalties as a principled alternative to purely likelihood-based criteria. Finally, developing open-source, production-grade implementations and broader biological benchmarks (beyond PPI) would further clarify when and how hierarchical aggregation best trades off accuracy, calibration, and memory/compute in heterogeneous classification problems.

B. Detailed Batch MM Algorithm

Inverse identities. For implementation, we use the block structure of [Equation \(5\)](#). In particular,

$$\mathbf{B}_{n,K-1}^{-1} = \left(\frac{4}{3} \mathbf{I}_{K-1} + \frac{8}{3(K-1)} \mathbf{1}_{K-1} \mathbf{1}_{K-1}^\top \right) \otimes \left(\sum_{n=1}^N \hat{\mathbf{x}}_n \hat{\mathbf{x}}_n^\top \right)^{-1}, \quad (11)$$

$$[\mathbf{B}_{n,M-1}^K]^{-1} = \mathbf{I}_K \otimes \mathbf{B}_{n,M-1}^{-1}. \quad (12)$$

In addition, for any diagonal matrix $\text{diag}(\mathbf{a})$ with positive entries, we have $\text{diag}(\mathbf{a})^{-1} = \text{diag}(1/\mathbf{a})$, which we apply to $\mathbf{Z}_n^{(t)}$ when needed.

Batch MM Algorithm for SGMLMoE. [Algorithm 2](#) implements a batch MM procedure for fitting SGMLMoE. At each iteration, it first computes responsibilities $\tau_{n,k}^{(t)}$ for all samples and experts using the current gate and expert probabilities, and then constructs the batch sufficient-statistic-like terms $(\mathbf{s}_n^{(t)}, \mathbf{r}_n^{(t)})$ together with the corresponding curvature blocks $(\mathbf{B}_{n,K}, \mathbf{B}_{n,M})$ that define the quadratic MM surrogate in [Equation \(6\)](#). These per-sample quantities are then aggregated over the batch to form global updates, including the diagonal weighting matrices $\mathbf{Z}_n^{(t)}$ and the gradients of the log-sum-exp terms g_n (gate) and e_n (experts). Finally, the method performs closed-form MM updates for the gate and expert parameters by solving two preconditioned linear systems, yielding $(\mathbf{w}^{(t+1)}, \mathbf{v}^{(t+1)})$. By construction, the resulting iterates monotonically improve the log-likelihood, and the routine terminates when the likelihood increment falls below the tolerance ε (or when

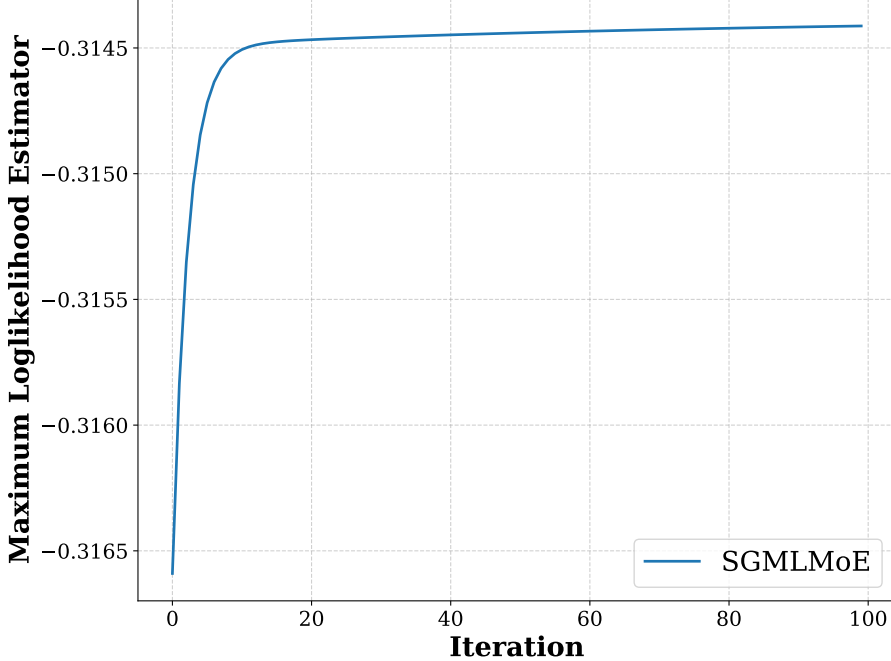


Figure 6. Evolution of the maximum log-likelihood for SGMLMoE over the first 100 optimization iterations with $N = 1000$.

the maximum number of iterations is reached).

C. Experimental Details

Real Dataset Pre-processing. We first use the dataset provided in (Tang et al., 2023b; Qi et al., 2007) to obtain positive interaction labels. Following Tang et al. (2023a), we adopt protein sequence data as inputs, collected from Consortium (2015), yielding 9,760 protein sequences. Each sequence is encoded as a 20-dimensional amino-acid composition vector using the ProtLearn library. We then restrict the dataset to proteins appearing in the DIP database, resulting in 2,321 proteins with retained identifiers and corresponding sequence encodings. To construct labeled interaction samples, we select n protein pairs with verified interactions in DIP and compute the element-wise absolute difference between their sequence encodings, producing 20-dimensional feature vectors labeled as 1. Similarly, we sample n non-interacting protein pairs absent from DIP and construct their feature vectors in the same manner, assigning label 0. The positive and negative samples are concatenated to form a $2n \times 20$ feature matrix with an associated binary label vector, and the resulting dataset is randomly shuffled prior to training.

Monotonicity of Maximum Loglikelihood Estimator. Classical optimization methods such as SGD and Adam often lead to unstable MLE behavior in mixture or Mixture-of-Experts models. This instability arises from the highly non-convex likelihood landscape, where inappropriate step sizes can cause oscillations or divergence, making performance sensitive to careful learning-rate tuning. Such tuning is problem-dependent and can be computationally costly, limiting robustness and reproducibility. In contrast, our proposed method avoids these issues by adopting an MM-based optimization scheme that guarantees monotonic improvement of the MLE objective, as established in Theorem 2. This monotonicity ensures stable and predictable optimization dynamics. We empirically illustrate this behavior by plotting the MLE trajectory across iterations in Figure 6. As shown, our method exhibits a smooth, non-decreasing likelihood progression, in contrast to the fluctuating behavior observed under gradient-based optimizers. The experiment is conducted on the synthetic dataset described in Section 5.2 with $N = 1000$ samples.

Surrogate function construction plays a pivotal role in optimization techniques such as MM algorithms. By leveraging mathematical inequalities, it is possible to approximate or bound complex objective functions with simpler, more tractable alternatives. Below are several fundamental inequalities commonly employed in the development of surrogate functions:

Algorithm 2 Batch MM Algorithm for SGMLMoE

Require: Batch data $\{(x_n, y_n)\}_{n=1}^N$, numbers of experts/classes (K, M) , polynomial degree D , initialization $\theta^{(0)} = (\mathbf{w}^{(0)}, \mathbf{v}^{(0)})$, tolerance $\varepsilon > 0$, maximum iterations T .

Ensure: MM iterates $\{\theta^{(t)}\}_{t \geq 0}$.

1: **for** $t = 0, 1, \dots, T - 1$ **do**

2: **E-step (Responsibilities).**

3: **for** $n = 1, \dots, N$ **do**

4: Form the feature vector $\hat{\mathbf{x}}_n = [x_{n,1}^0, \dots, x_{n,1}^D, \dots, x_{n,P}^0, \dots, x_{n,P}^D]^\top$.

5: Compute gate probabilities $\{\mathbf{g}_k(\mathbf{w}^{(t)}(\mathbf{x}_n))\}_{k=1}^K$.

6: Compute expert probabilities $\{\mathbf{e}_k(y_n = m; \mathbf{v}^{(t)}(\mathbf{x}_n))\}_{m=1}^M$ for each $k \in [K]$.

7: Compute posteriors

$$\tau_{n,k}^{(t)} = \frac{\mathbf{g}_k(\mathbf{w}^{(t)}(\mathbf{x}_n)) \mathbf{e}_k(y_n; \mathbf{v}^{(t)}(\mathbf{x}_n))}{\sum_{\ell=1}^K \mathbf{g}_\ell(\mathbf{w}^{(t)}(\mathbf{x}_n)) \mathbf{e}_\ell(y_n; \mathbf{v}^{(t)}(\mathbf{x}_n))}, \quad k \in [K].$$

8: Build $\mathbf{s}_n^{(t)}$ and $\mathbf{r}_n^{(t)}$ (using $\mathbb{1}(y_n, l)$ and the definitions in Equation (6) and the surrounding text).

9: Build the curvature blocks $\mathbf{B}_{n,K}$ and $\mathbf{B}_{n,M}$ (as in Equation (5)).

10: **end for**

11: **Aggregate Batch Quantities.**

12: $\mathbf{s}^{(t)} = \sum_{n=1}^N \mathbf{s}_n^{(t)}$, $\mathbf{r}^{(t)} = \sum_{n=1}^N \mathbf{r}_n^{(t)}$.

13: $\mathbf{B}_{n,K-1} = \sum_{n=1}^N \mathbf{B}_{n,K}$, $\mathbf{B}_{n,M-1} = \sum_{n=1}^N \mathbf{B}_{n,M}$, $\mathbf{B}_{n,M-1}^K = \mathbf{I}_K \otimes \mathbf{B}_{n,M-1}$.

14: **for** $n = 1, \dots, N$ **do**

15: Set $\boldsymbol{\tau}_{n,:}^{(t)} = [\tau_{n,1}^{(t)}, \dots, \tau_{n,K}^{(t)}]^\top$ and $\mathbf{Z}_n^{(t)} = \text{diag}(\boldsymbol{\tau}_{n,:}^{(t)} \otimes \mathbf{1}_{P(D+1)})$.

16: **end for**

17: **Compute Gradients of Log-sum-exp terms.**

18: $\nabla g(\mathbf{w}^{(t)}) = \sum_{n=1}^N \nabla g_n(\mathbf{w}^{(t)})$, where $g_n(\mathbf{w}) = \log\left(1 + \sum_{k=1}^{K-1} \exp(w_k(\mathbf{x}_n))\right)$.

19: For each $n \in [N]$, form $\nabla e_n(\mathbf{v}^{(t)}) = \text{vec}([\nabla e_n(\mathbf{c}_1^{(t)}), \dots, \nabla e_n(\mathbf{c}_K^{(t)})])$, where $e_n(\mathbf{c}_k) = \log\left(1 + \sum_{m=1}^{M-1} \exp(v_{m,k}(\mathbf{x}_n))\right)$.

20: **M-step (Closed-form MM Updates).**

21: Update the gate parameters:

$$\mathbf{w}^{(t+1)} = \mathbf{w}^{(t)} + \mathbf{B}_{n,K-1}^{-1} \left(\mathbf{s}^{(t)} - \nabla g(\mathbf{w}^{(t)}) \right).$$

22: Update the expert parameters:

$$\mathbf{v}^{(t+1)} = \mathbf{v}^{(t)} + \left(\sum_{n=1}^N \mathbf{Z}_n^{(t)} \mathbf{B}_{n,M-1}^K \right)^{-1} \left(\mathbf{r}^{(t)} - \sum_{n=1}^N \mathbf{Z}_n^{(t)} \nabla e_n(\mathbf{v}^{(t)}) \right).$$

23: Set $\theta^{(t+1)} = (\mathbf{w}^{(t+1)}, \mathbf{v}^{(t+1)})$.

24: **Stopping Criterion.** If $|\mathcal{L}(\theta^{(t+1)}) - \mathcal{L}(\theta^{(t)})| \leq \varepsilon$, **break**.

25: **end for**

D. Proofs of Main Results

D.1. Technical Contributions

Following the MM paradigm, we first propose a novel surrogate objective for SGMLMoE in [Theorem 1](#) and rigorously show that it satisfies the monotonicity property required by the MM algorithm in [Theorem 2](#). Building on this foundation, we turn to model merging and substantially modify the proof of Theorem 3.1 in [Nguyen et al. \(2024a\)](#) to accommodate our proposed Voronoi metric and the SGMLMoE framework, yielding the key inequality in [Theorem 3](#). Leveraging this result, we then follow the argument of Lemma 2 in [Do et al. \(2024\)](#) (see also [Thai et al. \(2025\)](#); [Hai et al. \(2026\)](#)) to derive an analogous monotone chain property for our model in [Theorem 4](#). Finally, we adapt the proofs of Theorems 1–3 in [Do et al. \(2024\)](#) for mixture models to our Voronoi loss and SGMLMoE setting, leading to theoretical guarantees on the convergence rate, model selection consistency, and merge convergence in [Theorem 5](#), [Theorem 6](#), and [Theorem 7](#), respectively.

D.2. Proof of Theorem 1

We derive the surrogate bound in [Equation \(6\)](#) by combining (i) a variational upper bound based on responsibilities (E-step) and (ii) a uniform quadratic majorization of the baseline log-sum-exp terms (MM step). We first recall the notation blocks used throughout this proof.

Batch Sufficient-statistics Notation. For each $n \in [N]$, define the gating-design vector in $\mathbb{R}^{(K-1)P(D+1)}$:

$$\mathbf{s}_n^{(t)} = [\tau_{n,1}^{(t)} x_{n,1}^0, \dots, \tau_{n,1}^{(t)} x_{n,1}^D, \dots, \tau_{n,K-1}^{(t)} x_{n,P}^D]^\top. \quad (13)$$

Define the expert-design vector $\mathbf{r}_n^{(t)}$ by stacking $r_{n,d,l,p,k}^{(t)} = \mathbb{1}(\mathbf{y}_n, l) \tau_{n,k}^{(t)} x_{n,p}^d$, $d \in \{0, \dots, D\}$, $l \in [M]$, $p \in [P]$, $k \in [K]$, into

$$\mathbf{r}_n^{(t)} = [r_{n,0,1,1,1}^{(t)}, \dots, r_{n,D,1,1,1}^{(t)}, \dots, r_{n,D,M,1,1}^{(t)}, \dots, r_{n,D,M,P,K}^{(t)}]^\top.$$

We also define the class-parameter blocks for each expert k by

$$\mathbf{c}_k = [\mathbf{v}_{1,k,0,1}, \dots, \mathbf{v}_{1,k,D,1}, \dots, \mathbf{v}_{M,k,D,1}, \dots, \mathbf{v}_{M,k,D,P}]^\top, \quad \mathbf{v} = \text{vec}([\mathbf{c}_1, \dots, \mathbf{c}_K]).$$

Finally, we aggregate the batch statistics as

$$\mathbf{s}^{(t)} = \sum_{n=1}^N \mathbf{s}_n^{(t)}, \quad \mathbf{r}^{(t)} = \sum_{n=1}^N \mathbf{r}_n^{(t)}.$$

Quadratic Majorizers for the Gate and Experts. For $k \in [K-1]$, let $w_k(\mathbf{x}) = \sum_{d=0}^D \omega_{k,d}^\top \mathbf{x}^d$ and define the gate log-sum-exp term

$$g_n(\mathbf{w}) = \log \left(1 + \sum_{k=1}^{K-1} \exp(w_k(\mathbf{x}_n)) \right).$$

For experts, define for each $k \in [K]$ the multinomial log-sum-exp term

$$e_n(\mathbf{c}_k) = \log \left(1 + \sum_{m=1}^{M-1} \exp(v_{m,k}(\mathbf{x}_n)) \right).$$

For any $K \in \mathbb{N}$, we use the quadratic majorizers based on the matrices

$$\mathbf{B}_{n,K} = \left(\frac{3}{4} \mathbf{I}_{K-1} - \frac{\mathbf{1}_{K-1} \mathbf{1}_{K-1}^\top}{2(K-1)} \right) \otimes \hat{\mathbf{x}}_n \hat{\mathbf{x}}_n^\top, \quad (14)$$

and similarly $\mathbf{B}_{n,M}$ is defined by replacing K with M in [Equation \(14\)](#). For compactness, introduce the centered increments $\bar{\mathbf{w}}_t = \mathbf{w} - \mathbf{w}^{(t)}$ and $\bar{\mathbf{c}}_{k,t} = \mathbf{c}_k - \mathbf{c}_k^{(t)}$. (Here $\hat{\mathbf{x}}_n = [x_{n,1}^0, \dots, x_{n,1}^D, \dots, x_{n,P}^0, \dots, x_{n,P}^D]^\top$.)

Step 1: Variational Upper Bound via Responsibilities. For each $n \in [N]$, define

$$a_{n,k}(\boldsymbol{\theta}) := \mathbf{g}_k(\mathbf{w}(\mathbf{x}_n)) \mathbf{e}_k(\mathbf{y}_n; \mathbf{v}(\mathbf{x}_n)), \quad s_{\boldsymbol{\theta}}(\mathbf{y}_n \mid \mathbf{x}_n) = \sum_{k=1}^K a_{n,k}(\boldsymbol{\theta}).$$

By the log-sum inequality (equivalently, Jensen's inequality / KL nonnegativity), for any $\boldsymbol{\tau}_{n,:} \in \Delta_K$,

$$-\log s_{\boldsymbol{\theta}}(\mathbf{y}_n \mid \mathbf{x}_n) \leq -\sum_{k=1}^K \tau_{n,k} \log a_{n,k}(\boldsymbol{\theta}) + \sum_{k=1}^K \tau_{n,k} \log \tau_{n,k}. \quad (15)$$

Choosing $\tau_{n,k} = \tau_{n,k}^{(t)} := a_{n,k}(\boldsymbol{\theta}^{(t)}) / \sum_{\ell} a_{n,\ell}(\boldsymbol{\theta}^{(t)})$ makes Equation (15) tight at $\boldsymbol{\theta} = \boldsymbol{\theta}^{(t)}$.

Expanding $\log a_{n,k}(\boldsymbol{\theta}) = \log \mathbf{g}_k(\mathbf{w}(\mathbf{x}_n)) + \log \mathbf{e}_k(\mathbf{y}_n; \mathbf{v}(\mathbf{x}_n))$ yields two convex log-sum-exp terms and linear contributions in the scores:

$$-\sum_{k=1}^K \tau_{n,k}^{(t)} \log \mathbf{g}_k(\mathbf{w}(\mathbf{x}_n)) = g_n(\mathbf{w}) - \sum_{k=1}^{K-1} \tau_{n,k}^{(t)} w_k(\mathbf{x}_n), \quad (16)$$

$$-\sum_{k=1}^K \tau_{n,k}^{(t)} \log \mathbf{e}_k(\mathbf{y}_n; \mathbf{v}(\mathbf{x}_n)) = \sum_{k=1}^K \tau_{n,k}^{(t)} e_n(\mathbf{c}_k) - \sum_{k=1}^K \tau_{n,k}^{(t)} \sum_{l=1}^M \mathbb{1}(\mathbf{y}_n, l) v_{l,k}(\mathbf{x}_n). \quad (17)$$

The linear terms in Equations (16) and (17) match the sufficient-statistics inner products $\mathbf{w}^\top \mathbf{s}_n^{(t)}$ and $\mathbf{v}^\top \mathbf{r}_n^{(t)}$ under the stacking conventions above (so that $w_k(\mathbf{x}_n) = \boldsymbol{\omega}_k^\top \hat{\mathbf{x}}_n$ and $v_{l,k}(\mathbf{x}_n) = \mathbf{v}_{l,k}^\top \hat{\mathbf{x}}_n$).

Collecting Equations (15) to (17) and summing over n gives

$$-\log s_{\boldsymbol{\theta}}(\mathbf{y} \mid \mathbf{x}) \leq C^{(t)} - \sum_{n=1}^N \mathbf{w}^\top \mathbf{s}_n^{(t)} - \sum_{n=1}^N \mathbf{v}^\top \mathbf{r}_n^{(t)} + \sum_{n=1}^N g_n(\mathbf{w}) + \sum_{n=1}^N \sum_{k=1}^K \tau_{n,k}^{(t)} e_n(\mathbf{c}_k), \quad (18)$$

where $C^{(t)} := \sum_{n=1}^N \sum_{k=1}^K \tau_{n,k}^{(t)} \log \tau_{n,k}^{(t)}$ does not depend on $\boldsymbol{\theta}$.

Step 2: Quadratic Majorization of g_n and e_n . Both g_n and e_n are baseline log-sum-exp functions composed with affine score maps. A standard calculation gives

$$\nabla^2 g_n(\mathbf{w}) = (\text{diag}(\hat{\mathbf{p}}_n) - \hat{\mathbf{p}}_n \hat{\mathbf{p}}_n^\top) \otimes \hat{\mathbf{x}}_n \hat{\mathbf{x}}_n^\top,$$

where $\hat{\mathbf{p}}_n$ are the baseline softmax probabilities over $k \in [K-1]$.

Applying Proposition 1 with $q = K-1$ (gate) and $q = M-1$ (expert), and then lifting the resulting Hessian bound through the linear score maps via Lemma 1, yields the quadratic majorizers in Equation (5). Indeed, by Lemma 1 (with $q = K-1$) and Proposition 1,

$$\nabla^2 g_n(\mathbf{w}) \preceq \mathbf{B}_{n,K},$$

with $\mathbf{B}_{n,K}$ defined in Equation (14). Therefore, the second-order Taylor formula along the segment between $\mathbf{w}^{(t)}$ and \mathbf{w} yields the global quadratic upper bound

$$g_n(\mathbf{w}) \leq g_n(\mathbf{w}^{(t)}) + \bar{\mathbf{w}}_t^\top \nabla g_n(\mathbf{w}^{(t)}) + \frac{1}{2} \bar{\mathbf{w}}_t^\top \mathbf{B}_{n,K} \bar{\mathbf{w}}_t, \quad \forall \mathbf{w}. \quad (19)$$

The same argument applies to $e_n(\mathbf{c}_k)$ (with $q = M-1$), giving for each $k \in [K]$,

$$e_n(\mathbf{c}_k) \leq e_n(\mathbf{c}_k^{(t)}) + \bar{\mathbf{c}}_{k,t}^\top \nabla e_n(\mathbf{c}_k^{(t)}) + \frac{1}{2} \bar{\mathbf{c}}_{k,t}^\top \mathbf{B}_{n,M} \bar{\mathbf{c}}_{k,t}, \quad \forall \mathbf{c}_k. \quad (20)$$

Step 3: Surrogate Bound. Plug Equations (19) and (20) into Equation (18) and absorb all terms that do not depend on θ into $C^{(t)}$. This yields exactly the surrogate inequality stated in Equation (6), namely

$$-\log s_\theta(y \mid x) \leq -\log [g(\theta, x_{[N]}, y_{[N]}; \theta^{(t)})],$$

with the explicit quadratic form in Equation (6). This completes the proof.

Lemma 1 (Kronecker product preserves Loewner order). *If $A \preceq B$ and $C \succeq 0$ are symmetric, then*

$$A \otimes C \preceq B \otimes C.$$

Proof of Lemma 1. Since $A \preceq B$, we have $B - A \succeq 0$. For any vector x ,

$$x^\top ((B - A) \otimes C)x = \|((B - A)^{1/2} \otimes C^{1/2})x\|^2 \geq 0,$$

so $(B - A) \otimes C \succeq 0$, which is equivalent to $A \otimes C \preceq B \otimes C$. \square

Proposition 1 (Uniform bound for baseline-softmax Hessian). *Let $q \in \mathbb{N}$ and let $\tilde{p} \in (0, 1)^{q+1}$ satisfy $\sum_{j=1}^{q+1} \tilde{p}_j = 1$. Write $\hat{p} = [\tilde{p}_1, \dots, \tilde{p}_q]^\top$ and $\Lambda = \text{diag}(\hat{p})$. Then*

$$\Lambda - \hat{p}\hat{p}^\top \preceq A_q := \frac{3}{4}I_q - \frac{\mathbf{1}_q \mathbf{1}_q^\top}{2q}.$$

Proof of Proposition 1. In this proof, we use the following definitions: $\mathbf{1}_{q+1} := (1, \dots, 1)^\top \in \mathbb{R}^{q+1}$, and $\mathbf{1}_{q+1}^\perp := \{\mathbf{u} \in \mathbb{R}^{q+1} : \mathbf{1}_{q+1}^\top \mathbf{u} = 0\}$.

Step 1: Full Simplex Covariance Bound. Define the $(q+1) \times (q+1)$ covariance-type matrix

$$W(\tilde{p}) = \text{diag}(\tilde{p}) - \tilde{p}\tilde{p}^\top.$$

Let $\mathbf{z} \in \{e_1, \dots, e_{q+1}\}$ be a one-hot random vector with $\mathbb{E}[\mathbf{z}] = \tilde{p}$. Then $W(\tilde{p}) = \text{Cov}(\mathbf{z})$ and for any \mathbf{u} ,

$$\mathbf{u}^\top W(\tilde{p}) \mathbf{u} = \text{Var}(\mathbf{u}^\top \mathbf{z}).$$

Since $\mathbf{u}^\top \mathbf{z}$ takes values in $\{\mathbf{u}_1, \dots, \mathbf{u}_{q+1}\}$, its range is at most

$$\max_{i,j} |\mathbf{u}_i - \mathbf{u}_j| = \max_{i,j} |\mathbf{u}^\top (e_i - e_j)| \leq \|\mathbf{u}\| \max_{i,j} \|e_i - e_j\| = \sqrt{2} \|\mathbf{u}\|.$$

By Popoviciu's inequality, $\text{Var}(\mathbf{u}^\top \mathbf{z}) \leq \frac{1}{4}(\text{range})^2 \leq \frac{1}{2} \|\mathbf{u}\|^2$. Hence $W(\tilde{p}) \preceq \frac{1}{2}I_{q+1}$. Moreover, $W(\tilde{p})\mathbf{1}_{q+1} = \mathbf{0}$, so $W(\tilde{p})$ is supported on $\mathbf{1}_{q+1}^\perp$, and therefore

$$W(\tilde{p}) \preceq \frac{1}{2} \left(I_{q+1} - \frac{\mathbf{1}_{q+1} \mathbf{1}_{q+1}^\top}{q+1} \right).$$

Step 2: Take the Principal Submatrix. The top-left $q \times q$ principal submatrix of $W(\tilde{p})$ is exactly $\Lambda - \hat{p}\hat{p}^\top$. Taking the corresponding principal submatrix of the right-hand side yields

$$\Lambda - \hat{p}\hat{p}^\top \preceq \frac{1}{2} \left(I_q - \frac{\mathbf{1}_q \mathbf{1}_q^\top}{q+1} \right).$$

Step 3: Loosen to A_q Used in Equation (5). It remains to show $\frac{1}{2}(I_q - \frac{\mathbf{1}_q \mathbf{1}_q^\top}{q+1}) \preceq \frac{3}{4}I_q - \frac{\mathbf{1}_q \mathbf{1}_q^\top}{2q}$. Their difference equals

$$\left(\frac{3}{4} - \frac{1}{2} \right) I_q - \left(\frac{1}{2q} - \frac{1}{2(q+1)} \right) \mathbf{1}_q \mathbf{1}_q^\top = \frac{1}{4} I_q - \frac{1}{2q(q+1)} \mathbf{1}_q \mathbf{1}_q^\top,$$

whose eigenvalues are $\frac{1}{4}$ on $\mathbf{1}_q^\perp$ and $\frac{1}{4} - \frac{q}{2q(q+1)} = \frac{q-1}{4(q+1)} \geq 0$ along $\mathbf{1}_q$. Thus the difference is positive semidefinite, proving the claim. \square

D.3. Proof of Theorem 2: Verification of MM Properties for Algorithm 1

Throughout this proof we use the notation and building blocks introduced in Section D.2, in particular the batch sufficient-statistics $s_n^{(t)}$, $r_n^{(t)}$ in Equation (4) and the quadratic curvature matrices $B_{n,K}$, $B_{n,M}$ in Equation (5). Let $\mathcal{L}(\theta) = \sum_{n=1}^N \log s_\theta(y_n | \mathbf{x}_n)$ be the observed-data log-likelihood.

Step 1: MM Majorization and Tangency (from Theorem 1). Define the batch surrogate $\mathcal{S}(\theta, \theta^{(t)})$ for $-\mathcal{L}(\theta)$ by the right-hand side of Equation (6) (absorbing all terms independent of θ into a constant). By Theorem 1, for every iterate $\theta^{(t)}$ the surrogate satisfies the MM conditions

$$-\mathcal{L}(\theta) \leq \mathcal{S}(\theta, \theta^{(t)}) \quad \forall \theta, \quad -\mathcal{L}(\theta^{(t)}) = \mathcal{S}(\theta^{(t)}, \theta^{(t)}). \quad (21)$$

Step 2: Exact Minimization of the Surrogate by Algorithm 1. Fix $\theta^{(t)}$ and use the centered increments $\bar{w}_t = \mathbf{w} - \mathbf{w}^{(t)}$ and $\bar{c}_{k,t} = \mathbf{c}_k - \mathbf{c}_k^{(t)}$ as in Section D.2. Since the surrogate is the sum of (i) a gate quadratic term in \mathbf{w} and (ii) K independent expert quadratics in $\{\mathbf{c}_k\}_{k=1}^K$, it decomposes as

$$\mathcal{S}(\theta, \theta^{(t)}) = C^{(t)} + \mathcal{S}_g(\mathbf{w}; \theta^{(t)}) + \sum_{k=1}^K \mathcal{S}_{e,k}(\mathbf{c}_k; \theta^{(t)}),$$

where $C^{(t)}$ does not depend on θ , and (up to additive constants)

$$\mathcal{S}_g(\mathbf{w}; \theta^{(t)}) = -\mathbf{w}^\top \mathbf{s}^{(t)} + \sum_{n=1}^N \left\{ \nabla g_n(\mathbf{w}^{(t)})^\top \bar{w}_t + \frac{1}{2} \bar{w}_t^\top B_{n,K} \bar{w}_t \right\}, \quad (22)$$

$$\mathcal{S}_{e,k}(\mathbf{c}_k; \theta^{(t)}) = -\mathbf{c}_k^\top \mathbf{r}_k^{(t)} + \sum_{n=1}^N \tau_{n,k}^{(t)} \left\{ \nabla e_n(\mathbf{c}_k^{(t)})^\top \bar{c}_{k,t} + \frac{1}{2} \bar{c}_{k,t}^\top B_{n,M} \bar{c}_{k,t} \right\}. \quad (23)$$

Here $\mathbf{s}^{(t)} = \sum_{n=1}^N s_n^{(t)}$, $\mathbf{r}^{(t)} = \sum_{n=1}^N \mathbf{r}_n^{(t)}$, and $\mathbf{r}_k^{(t)}$ is the block of $\mathbf{r}^{(t)}$ corresponding to expert k (under the stacking convention defining $\mathbf{v} = \text{vec}([\mathbf{c}_1, \dots, \mathbf{c}_K])$).

Introduce the aggregated curvatures and gradients

$$\begin{aligned} \mathbf{B}_{K-1} &:= \sum_{n=1}^N \mathbf{B}_{n,K}, & \mathbf{B}_{M-1,k}^{(t)} &:= \sum_{n=1}^N \tau_{n,k}^{(t)} \mathbf{B}_{n,M}, \\ \nabla g(\mathbf{w}^{(t)}) &:= \sum_{n=1}^N \nabla g_n(\mathbf{w}^{(t)}), & \nabla e_k^{(t)} &:= \sum_{n=1}^N \tau_{n,k}^{(t)} \nabla e_n(\mathbf{c}_k^{(t)}). \end{aligned}$$

Then Equation (22) is a (strictly) convex quadratic in \mathbf{w} whenever $\mathbf{B}_{K-1} \succ \mathbf{0}$, and differentiating yields

$$\nabla_{\mathbf{w}} \mathcal{S}_g(\mathbf{w}; \theta^{(t)}) = -\mathbf{s}^{(t)} + \nabla g(\mathbf{w}^{(t)}) + \mathbf{B}_{K-1}(\mathbf{w} - \mathbf{w}^{(t)}).$$

Setting this to $\mathbf{0}$ gives the unique minimizer

$$\mathbf{w}^{(t+1)} = \mathbf{w}^{(t)} + \mathbf{B}_{K-1}^{-1}(\mathbf{s}^{(t)} - \nabla g(\mathbf{w}^{(t)})), \quad (24)$$

which matches the gate update in Algorithm 1 (up to the same aggregation notation).

Similarly, for each $k \in [K]$, Equation (23) is a convex quadratic in \mathbf{c}_k and

$$\nabla_{\mathbf{c}_k} \mathcal{S}_{e,k}(\mathbf{c}_k; \theta^{(t)}) = -\mathbf{r}_k^{(t)} + \nabla e_k^{(t)} + \mathbf{B}_{M-1,k}^{(t)}(\mathbf{c}_k - \mathbf{c}_k^{(t)}).$$

Setting this to $\mathbf{0}$ yields

$$\mathbf{c}_k^{(t+1)} = \mathbf{c}_k^{(t)} + (\mathbf{B}_{M-1,k}^{(t)})^{-1}(\mathbf{r}_k^{(t)} - \nabla e_k^{(t)}), \quad k \in [K], \quad (25)$$

equivalent to the expert update in Algorithm 1 (the algorithm writes this in a vectorized form). Since \mathcal{S} decomposes across the gate block and expert blocks, the concatenation $\theta^{(t+1)} = (\mathbf{w}^{(t+1)}, \mathbf{v}^{(t+1)})$ satisfies

$$\theta^{(t+1)} \in \arg \min_{\theta} \mathcal{S}(\theta, \theta^{(t)}). \quad (26)$$

If some curvature matrix is singular, the same first-order conditions hold using the Moore–Penrose pseudoinverse, or by adding a small ridge $\lambda \mathbf{I}$; in either case the MM validity in Equation (21) is unchanged.

Step 3: Monotonicity (MM Ascent). By exact minimization Equation (26),

$$\mathcal{S}(\boldsymbol{\theta}^{(t+1)}, \boldsymbol{\theta}^{(t)}) \leq \mathcal{S}(\boldsymbol{\theta}^{(t)}, \boldsymbol{\theta}^{(t)}).$$

By tangency in Equation (21), $\mathcal{S}(\boldsymbol{\theta}^{(t)}, \boldsymbol{\theta}^{(t)}) = -\mathcal{L}(\boldsymbol{\theta}^{(t)})$. By majorization in Equation (21) evaluated at $\boldsymbol{\theta} = \boldsymbol{\theta}^{(t+1)}$, $-\mathcal{L}(\boldsymbol{\theta}^{(t+1)}) \leq \mathcal{S}(\boldsymbol{\theta}^{(t+1)}, \boldsymbol{\theta}^{(t)})$. Combining the three displays yields

$$-\mathcal{L}(\boldsymbol{\theta}^{(t+1)}) \leq -\mathcal{L}(\boldsymbol{\theta}^{(t)}) \iff \mathcal{L}(\boldsymbol{\theta}^{(t+1)}) \geq \mathcal{L}(\boldsymbol{\theta}^{(t)}),$$

which proves Theorem 2.

D.4. Proof of Theorem 3

This result extends the inverse-inequality technique developed in Nguyen et al. (2024a) to our SGMLMoE parameterization with polynomial score functions. Throughout, we use the lifted feature $\hat{\mathbf{x}} = \phi_D(\mathbf{x}) \in \hat{\mathbb{X}} \subset \mathbb{R}^{PD}$ and the identifiable mixing-measure representation introduced in Section 4.2–Section 4.3.

Recall that for $G = \sum_{l=1}^K \pi_l \delta_{\eta_l} \in \mathcal{O}_K(\mathbb{T})$ and $G_0 = \sum_{k=1}^{K_0} \pi_k^0 \delta_{\eta_k^0} \in \mathcal{O}_{K_0}(\mathbb{T})$, we write $s_G(y \mid \mathbf{x}) = \sum_{l=1}^K \mathbf{g}_l(\mathbf{x}; G) \mathbf{e}_l(y \mid \mathbf{x}; G)$, and we use the covariate-averaged TV discrepancy $\mathcal{D}_{\text{TV}}(s_G, s_{G_0}) = \mathbb{E}_{\mathbf{x}}[\mathcal{D}_{\text{TV}}(s_G(\cdot \mid \mathbf{x}), s_{G_0}(\cdot \mid \mathbf{x}))]$.

We prove the local and global parts separately.

Local Structure. We show the following local inverse inequality:

$$\liminf_{\varepsilon \rightarrow 0} \inf_{\substack{G \in \mathcal{O}_K(\mathbb{T}): \\ \mathcal{D}_{\text{V}}(G, G_0) \leq \varepsilon}} \frac{\mathcal{D}_{\text{TV}}(s_G, s_{G_0})}{\mathcal{D}_{\text{V}}(G, G_0)} > 0. \quad (27)$$

Assume by contradiction that Equation (27) fails. Then there exists a sequence $G^{(r)} = \sum_{l=1}^K \pi_l^{(r)} \delta_{\eta_l^{(r)}} \in \mathcal{O}_K(\mathbb{T})$ such that

$$\mathcal{D}_{\text{V}}(G^{(r)}, G_0) \rightarrow 0 \quad \text{and} \quad \frac{\mathcal{D}_{\text{TV}}(s_{G^{(r)}}, s_{G_0})}{\mathcal{D}_{\text{V}}(G^{(r)}, G_0)} \rightarrow 0 \quad (r \rightarrow \infty). \quad (28)$$

For r large, the Voronoi partition $\{\mathbb{V}_k\}_{k=1}^{K_0}$ is well-defined as in Section 4.3. For $l \in \mathbb{V}_k$, write the local differences $\Delta\hat{\omega}_{lk}^{(r)} = \hat{\omega}_l^{(r)} - \hat{\omega}_k^0$, $\Delta\bar{v}_{lkm}^{(r)} = \bar{v}_{m,l}^{(r)} - \bar{v}_{m,k}^0$, $\Delta\hat{v}_{lkm}^{(r)} = \hat{v}_{m,l}^{(r)} - \hat{v}_{m,k}^0$ for $m \in [M-1]$, and $\Delta\pi_k^{(r)} = \sum_{l \in \mathbb{V}_k} \pi_l^{(r)} - \pi_k^0$. By Equation (7) and $\mathcal{D}_{\text{V}}(G^{(r)}, G_0) \rightarrow 0$, all these quantities vanish.

Step 1: Finite Taylor Representation. Define the true gate normalizer $Z_0(\hat{\mathbf{x}}) := \sum_{k=1}^{K_0} \pi_k^0 \exp((\hat{\omega}_k^0)^\top \hat{\mathbf{x}})$. For each class $m \in [M]$, consider the rescaled difference

$$T_r(m, \hat{\mathbf{x}}) := Z_0(\hat{\mathbf{x}}) \left(s_{G^{(r)}}(m \mid \hat{\mathbf{x}}) - s_{G_0}(m \mid \hat{\mathbf{x}}) \right). \quad (29)$$

Using the softmax form for $\mathbf{g}_l(\cdot; G)$ and the multinomial-logistic form for $\mathbf{e}_l(\cdot \mid \cdot; G)$, a Taylor expansion around each true atom η_k^0 yields the decomposition

$$T_r(m, \hat{\mathbf{x}}) = \sum_{k=1}^{K_0} \sum_{\xi \in \Xi_k} A_{k,\xi}^{(r)} \Psi_{k,\xi}(m, \hat{\mathbf{x}}) + R_r(m, \hat{\mathbf{x}}), \quad (30)$$

where: (i) $\{\Psi_{k,\xi}(m, \hat{\mathbf{x}})\}$ is a *finite* collection of analytic basis functions of the form

$$\hat{\mathbf{x}}^\alpha \exp((\hat{\omega}_k^0)^\top \hat{\mathbf{x}}) \partial^\beta \mathbf{e}(m \mid \hat{\mathbf{x}}; \bar{v}_k^0, \hat{v}_k^0),$$

with multi-indices (α, β) of bounded total order (first order when $|\mathbb{V}_k| = 1$, and up to second order when $|\mathbb{V}_k| > 1$); (ii) the coefficients $A_{k,\xi}^{(r)}$ are explicit finite sums over $l \in \mathbb{V}_k$ of monomials in $\Delta\hat{\omega}_{lk}^{(r)}$, $\Delta\bar{v}_{lkm}^{(r)}$, $\Delta\hat{v}_{lkm}^{(r)}$, and $\Delta\pi_k^{(r)}$, weighted by $\pi_l^{(r)}$; (iii) the remainder satisfies

$$\sup_{m \in [M]} \mathbb{E}_{\mathbf{x}}[|R_r(m, \phi_D(\mathbf{x}))|] = o(\mathcal{D}_{\text{V}}(G^{(r)}, G_0)), \quad (r \rightarrow \infty). \quad (31)$$

Step 2: Some Normalized Coefficient Must be Non-vanishing. Let

$$m_r := \max_{k,\xi} \frac{|A_{k,\xi}^{(r)}|}{\mathcal{D}_V(G^{(r)}, G_0)}.$$

We claim $\liminf_{r \rightarrow \infty} m_r > 0$. If instead $m_r \rightarrow 0$, then all coefficients in Equation (30) would satisfy $|A_{k,\xi}^{(r)}| = o(\mathcal{D}_V(G^{(r)}, G_0))$. But the collection of coefficients $\{A_{k,\xi}^{(r)}\}$ contains, by construction, the same first- and second-order weighted increments that appear in Equation (7): for cells $|\mathbb{V}_k| = 1$ it contains the weighted linear terms $\sum_{l \in \mathbb{V}_k} \pi_l^{(r)} \|\Delta \hat{\omega}_{lk}^{(r)}\|$, $\sum_{l \in \mathbb{V}_k} \pi_l^{(r)} |\Delta \bar{v}_{lkm}^{(r)}|$, $\sum_{l \in \mathbb{V}_k} \pi_l^{(r)} \|\Delta \hat{v}_{lkm}^{(r)}\|$, and for cells $|\mathbb{V}_k| > 1$ it contains the weighted quadratic terms $\sum_{l \in \mathbb{V}_k} \pi_l^{(r)} \|\Delta \hat{\omega}_{lk}^{(r)}\|^2$, $\sum_{l \in \mathbb{V}_k} \pi_l^{(r)} |\Delta \bar{v}_{lkm}^{(r)}|^2$, $\sum_{l \in \mathbb{V}_k} \pi_l^{(r)} \|\Delta \hat{v}_{lkm}^{(r)}\|^2$, as well as the mass discrepancy terms $|\Delta \pi_k^{(r)}|$. Therefore $m_r \rightarrow 0$ would force $\mathcal{D}_V(G^{(r)}, G_0) = o(\mathcal{D}_V(G^{(r)}, G_0))$, a contradiction. Hence $\liminf_{r \rightarrow \infty} m_r > 0$.

Step 3: Fatou and Linear Independence Gives a Contradiction. Divide Equation (30) by $m_r \mathcal{D}_V(G^{(r)}, G_0)$ and take covariate expectation. Using Equation (28), the definition Equation (29), and Equation (31), we obtain

$$\mathbb{E}_{\mathbf{x}} \left[\sum_{m=1}^M \frac{|T_r(m, \phi_D(\mathbf{x}))|}{m_r \mathcal{D}_V(G^{(r)}, G_0)} \right] \rightarrow 0.$$

By Fatou's lemma, for each $m \in [M]$ we can extract a subsequence (not relabeled) such that

$$\frac{T_r(m, \hat{\mathbf{x}})}{m_r \mathcal{D}_V(G^{(r)}, G_0)} \rightarrow 0 \quad \text{for a.e. } \hat{\mathbf{x}} \in \hat{\mathbb{X}}.$$

Along this subsequence, the normalized coefficients converge (by boundedness) to limits $a_{k,\xi} = \lim_{r \rightarrow \infty} A_{k,\xi}^{(r)} / (m_r \mathcal{D}_V(G^{(r)}, G_0))$, with at least one $a_{k,\xi} \neq 0$ because $\liminf m_r > 0$. Passing to the limit in Equation (30) yields, for each $m \in [M]$ and a.e. $\hat{\mathbf{x}}$,

$$\sum_{k=1}^{K_0} \sum_{\xi \in \Xi_k} a_{k,\xi} \Psi_{k,\xi}(m, \hat{\mathbf{x}}) = 0. \quad (32)$$

Finally, by identifiability of the SGMLMoE and the fact that $\hat{\omega}_1^0, \dots, \hat{\omega}_{K_0}^0$ are distinct, the family of analytic functions $\{\Psi_{k,\xi}(m, \cdot)\}_{k,\xi}$ is linearly independent on $\hat{\mathbb{X}}$. Thus Equation (32) forces all $a_{k,\xi} = 0$, contradicting that at least one is nonzero. This contradiction establishes the local bound Equation (27).

Global Structure. By the local result, there exists $\varepsilon' > 0$ and $c' > 0$ such that

$$\mathcal{D}_{\text{TV}}(s_G, s_{G_0}) \geq c' \mathcal{D}_V(G, G_0) \quad \text{whenever } \mathcal{D}_V(G, G_0) \leq \varepsilon'.$$

It remains to prove the complementary bound on the set $\{G \in \mathcal{O}_K(\mathbb{T}) : \mathcal{D}_V(G, G_0) \geq \varepsilon'\}$:

$$\inf_{\substack{G \in \mathcal{O}_K(\mathbb{T}): \\ \mathcal{D}_V(G, G_0) \geq \varepsilon'}} \frac{\mathcal{D}_{\text{TV}}(s_G, s_{G_0})}{\mathcal{D}_V(G, G_0)} > 0. \quad (33)$$

Assume Equation (33) fails. Then there exists $G'^{(r)} \in \mathcal{O}_K(\mathbb{T})$ such that $\mathcal{D}_V(G'^{(r)}, G_0) \geq \varepsilon'$ and $\mathcal{D}_{\text{TV}}(s_{G'^{(r)}}, s_{G_0}) \rightarrow 0$. Under the standing compactness assumption on \mathbb{T} (hence on $\mathcal{O}_K(\mathbb{T})$ in the weak topology), extract a subsequence with $G'^{(r)} \Rightarrow G'$ for some $G' \in \mathcal{O}_K(\mathbb{T})$. By continuity of $G \mapsto s_G(\cdot \mid \mathbf{x})$ and dominated convergence, $\mathcal{D}_{\text{TV}}(s_{G'}, s_{G_0}) = 0$, hence $s_{G'}(\cdot \mid \mathbf{x}) = s_{G_0}(\cdot \mid \mathbf{x})$ for a.e. \mathbf{x} . By identifiability of SGMLMoE, this implies $G' \equiv G_0$, contradicting $\mathcal{D}_V(G'^{(r)}, G_0) \geq \varepsilon'$. Therefore Equation (33) holds, and combining local and global parts yields Equation (8). This completes the proof.

D.5. Proof of Theorem 4

We prove the first link of the chain, $\mathcal{D}_V(G^{(K)}, G_0) \gtrsim \mathcal{D}_V(G^{(K-1)}, G_0)$, since the remaining inequalities follow by repeating the same argument at each merge step.

Throughout, we write a generic K -atom measure as

$$G = \sum_{l=1}^K \pi_l \delta_{\eta_l}, \quad \pi_l = \exp(\bar{\omega}_l), \quad \eta_l = \left(\hat{\omega}_l, \bar{\omega}_l, \{(\hat{v}_{m,l}, \bar{v}_{m,l})\}_{m=1}^{M-1} \right) \in \mathbb{T},$$

and we use the Voronoi partition $\{\mathbb{V}_k\}_{k=1}^{K_0}$ induced by G_0 as in Section 4.3. For $l \in \mathbb{V}_k$, recall the parameter gaps $\Delta\hat{\omega}_{lk} = \hat{\omega}_l - \hat{\omega}_k^0$, $\Delta\bar{v}_{lkm} = \bar{v}_{m,l} - \bar{v}_{m,k}^0$, $\Delta\hat{v}_{lkm} = \hat{v}_{m,l} - \hat{v}_{m,k}^0$ for $m \in [M-1]$.

Step 1: the Closest Pair Lies in a Common Voronoi Cell. Let $G^{(K)}$ be sufficiently close to G_0 so that the Voronoi cells \mathbb{V}_k are well-defined and stable. Since the merge rule in Equation (9) uses squared Euclidean dissimilarities in $\hat{\omega}$ and $(\bar{v}_m, \hat{v}_m)_{m \in [M-1]}$, any pair of atoms belonging to different Voronoi cells stays separated by a fixed positive amount (depending only on G_0 and the local metric on \mathbb{T}), whereas within-cell pairs can be arbitrarily close when over-fitting occurs. Consequently, for $G^{(K)}$ close enough to G_0 , the minimizing pair in $h^{(K)} = \min_{l \neq l'} d(\pi_l \delta_{\eta_l}, \pi_{l'} \delta_{\eta_{l'}})$ must belong to the same cell \mathbb{V}_k . Fix such a cell and denote it by \mathbb{V}_{k^*} , and assume the merged indices are $(l_1, l_2) \subset \mathbb{V}_{k^*}$.

Step 2: Notation for the Merge. Let $G^{(K-1)}$ be obtained from $G^{(K)}$ by merging atoms l_1 and l_2 according to Equation (10). Write the merged atom as (π_*, η_*) , where

$$\pi_* = \pi_{l_1} + \pi_{l_2}, \quad \hat{\omega}_* = \frac{\pi_{l_1}}{\pi_*} \hat{\omega}_{l_1} + \frac{\pi_{l_2}}{\pi_*} \hat{\omega}_{l_2},$$

and, for each $m \in [M-1]$,

$$\bar{v}_{m,*} = \frac{\pi_{l_1}}{\pi_*} \bar{v}_{m,l_1} + \frac{\pi_{l_2}}{\pi_*} \bar{v}_{m,l_2}, \quad \hat{v}_{m,*} = \frac{\pi_{l_1}}{\pi_*} \hat{v}_{m,l_1} + \frac{\pi_{l_2}}{\pi_*} \hat{v}_{m,l_2}.$$

All other atoms are unchanged. Since $l_1, l_2 \in \mathbb{V}_{k^*}$ and $G^{(K)}$ is close to G_0 , the merged atom also remains assigned to the same cell \mathbb{V}_{k^*} .

Step 3: the Voronoi Weight-mismatch Term is Preserved. For each $k \in [K_0]$, the weight-mismatch contribution $|\sum_{l \in \mathbb{V}_k} \pi_l - \pi_k^0|$ is unchanged by merging within \mathbb{V}_k : indeed, for $k \neq k^*$ nothing changes, and for $k = k^*$,

$$\sum_{l \in \mathbb{V}_{k^*}} \pi_l = \sum_{l \in \mathbb{V}_{k^*} \setminus \{l_1, l_2\}} \pi_l + \pi_{l_1} + \pi_{l_2} = \sum_{l \in \mathbb{V}_{k^*} \setminus \{l_1, l_2\}} \pi_l + \pi_*,$$

so the absolute deviation from $\pi_{k^*}^0$ is identical before and after merging.

Step 4: Within-cell Quadratic Terms Decrease under Barycentric Merging. Consider first the gate-slope quadratic term on the over-covered cell $|\mathbb{V}_{k^*}| > 1$:

$$\sum_{l \in \mathbb{V}_{k^*}} \pi_l \|\Delta\hat{\omega}_{lk^*}\|^2 = \sum_{l \in \mathbb{V}_{k^*} \setminus \{l_1, l_2\}} \pi_l \|\Delta\hat{\omega}_{lk^*}\|^2 + \pi_{l_1} \|\Delta\hat{\omega}_{l_1 k^*}\|^2 + \pi_{l_2} \|\Delta\hat{\omega}_{l_2 k^*}\|^2.$$

By convexity of $u \mapsto \|u\|^2$ and the definition $\Delta\hat{\omega}_{*k^*} = \frac{\pi_{l_1}}{\pi_*} \Delta\hat{\omega}_{l_1 k^*} + \frac{\pi_{l_2}}{\pi_*} \Delta\hat{\omega}_{l_2 k^*}$, we have the Jensen inequality

$$\pi_{l_1} \|\Delta\hat{\omega}_{l_1 k^*}\|^2 + \pi_{l_2} \|\Delta\hat{\omega}_{l_2 k^*}\|^2 \geq \pi_* \|\Delta\hat{\omega}_{*k^*}\|^2.$$

Hence,

$$\sum_{l \in \mathbb{V}_{k^*}} \pi_l \|\Delta\hat{\omega}_{lk^*}\|^2 \geq \sum_{l \in \mathbb{V}_{k^*} \setminus \{l_1, l_2\}} \pi_l \|\Delta\hat{\omega}_{lk^*}\|^2 + \pi_* \|\Delta\hat{\omega}_{*k^*}\|^2,$$

which is exactly the corresponding contribution after merging l_1, l_2 into $*$.

The same argument applies to each expert block, for every $m \in [M - 1]$: since $u \mapsto |u|^2$ and $u \mapsto \|u\|^2$ are convex,

$$\begin{aligned} \pi_{l_1} |\Delta \bar{v}_{l_1 k^* m}|^2 + \pi_{l_2} |\Delta \bar{v}_{l_2 k^* m}|^2 &\geq \pi_* |\Delta \bar{v}_{* k^* m}|^2, \\ \pi_{l_1} \|\Delta \hat{v}_{l_1 k^* m}\|^2 + \pi_{l_2} \|\Delta \hat{v}_{l_2 k^* m}\|^2 &\geq \pi_* \|\Delta \hat{v}_{* k^* m}\|^2, \end{aligned}$$

and therefore the entire within-cell quadratic contribution in Equation (7) for cell \mathbb{V}_{k^*} does not increase after merging.

Step 5: Conclusion. All other cells are unaffected, and the linear (single-covered) terms in $\mathcal{D}_E(G, G_0)$ are unchanged because they depend only on weights and on singletons. Hence,

$$\mathcal{D}_V(G^{(K)}, G_0) \gtrsim \mathcal{D}_V(G^{(K-1)}, G_0),$$

with an absolute constant (in particular, one may take the implicit constant to be 1 in the within-cell comparison). Iterating the same argument along the successive merges yields the full chain claimed in Theorem 4. \square

D.6. Proof of Theorem 5

Throughout, implicit constants in \lesssim, \gtrsim are universal and may change line to line.

Wasserstein Distance for Finite Mixing Measures. For two mixing measures

$$G = \sum_{l=1}^K \pi_l \delta_{\eta_l}, \quad G' = \sum_{l'=1}^{K'} \pi'_{l'} \delta_{\eta'_{l'}},$$

and any $r \geq 1$, define the Wasserstein- r distance

$$W_r(G, G') = \left(\inf_{Q \in \Pi(\pi, \pi')} \sum_{l=1}^K \sum_{l'=1}^{K'} Q_{ll'} \|\eta_l - \eta'_{l'}\|^r \right)^{1/r},$$

where $\Pi(\pi, \pi')$ is the set of couplings between $\pi = (\pi_1, \dots, \pi_K)$ and $\pi' = (\pi'_1, \dots, \pi'_{K'})$, i.e.,

$$\Pi(\pi, \pi') = \left\{ Q \in \mathbb{R}_+^{K \times K'} : \sum_{l'=1}^{K'} Q_{ll'} = \pi_l, \sum_{l=1}^K Q_{ll'} = \pi'_{l'}, \forall l \in [K], l' \in [K'] \right\}.$$

A Useful Lower Bound (Wasserstein Controls Componentwise Discrepancy). Fix the true mixing measure $G_0 = \sum_{k=1}^{K_0} \pi_k^0 \delta_{\eta_k^0} \in \mathcal{O}_{K_0}(\mathbb{T})$ and consider $G = \sum_{l=1}^K \pi_l \delta_{\eta_l} \in \mathcal{O}_K(\mathbb{T})$ such that $W_r(G, G_0) \rightarrow 0$. Then (see, e.g., (Ho & Nguyen, 2019)) there exists a Voronoi assignment $l \mapsto k(l) \in [K_0]$ and cells $\mathbb{V}_k = \{l \in [K] : k(l) = k\}$ such that

$$W_r^r(G, G_0) \gtrsim \sum_{k=1}^{K_0} \left(\left| \sum_{l \in \mathbb{V}_k} \pi_l - \pi_k^0 \right| + \sum_{l \in \mathbb{V}_k} \pi_l \|\eta_l - \eta_k^0\|^r \right). \quad (34)$$

Part 1: Voronoi and Height Rates on Over-fitted Levels $\kappa \in \{K_0 + 1, \dots, K\}$. Let

$$A_N := \left\{ \mathcal{D}_{\text{TV}}(s_{\hat{G}_N}, s_{G_0}) \leq C \sqrt{\log N/N} \right\},$$

where $C > 0$ is the constant from Fact 1. By Fact 1, $\mathbb{P}(A_N) \geq 1 - c_1 N^{-c_2}$. On A_N , combining Theorem 3 with the density bound yields

$$\mathcal{D}_V(\hat{G}_N, G_0) \lesssim \sqrt{\log N/N}. \quad (35)$$

Next, by Theorem 4, the Voronoi loss is monotone (up to constants) along the merge chain, hence for each $\kappa \in \{K_0 + 1, \dots, K\}$,

$$\mathcal{D}_V(\hat{G}_N^{(\kappa)}, G_0) \lesssim \sqrt{\log N/N}. \quad (36)$$

We now bound the dendrogram height $h_N^{(\kappa)}$ for $\kappa \geq K_0 + 1$. Since $\kappa > K_0$, at level κ there exists at least one Voronoi cell containing two distinct atoms of $\widehat{G}_N^{(\kappa)}$. Fix such a cell \mathbb{V}_{k^*} and pick two distinct indices $l_1 \neq l_2 \in \mathbb{V}_{k^*}$. Write $\widehat{G}_N^{(\kappa)} = \sum_{l=1}^{\kappa} \pi_l^{(\kappa)} \delta_{\eta_l^{(\kappa)}}$ and abbreviate $\pi_l := \pi_l^{(\kappa)}$, $\eta_l := \eta_l^{(\kappa)}$. From the definition of \mathcal{D}_V in Equation (7) and Equation (36), we obtain

$$\begin{aligned} & \pi_{l_1} \left(\|\hat{\omega}_{l_1} - \hat{\omega}_{k^*}^0\|^2 + \sum_{m=1}^{M-1} (|\bar{v}_{m,l_1} - \bar{v}_{m,k^*}^0|^2 + \|\hat{v}_{m,l_1} - \hat{v}_{m,k^*}^0\|^2) \right) \\ & + \pi_{l_2} \left(\|\hat{\omega}_{l_2} - \hat{\omega}_{k^*}^0\|^2 + \sum_{m=1}^{M-1} (|\bar{v}_{m,l_2} - \bar{v}_{m,k^*}^0|^2 + \|\hat{v}_{m,l_2} - \hat{v}_{m,k^*}^0\|^2) \right) \lesssim \sqrt{\log N/N}. \end{aligned} \quad (37)$$

Using the elementary inequality

$$\min\{\pi_{l_1}, \pi_{l_2}\} \geq \frac{\pi_{l_1} \pi_{l_2}}{\pi_{l_1} + \pi_{l_2}},$$

and the triangle inequality $\|\hat{\omega}_{l_1} - \hat{\omega}_{l_2}\| \leq \|\hat{\omega}_{l_1} - \hat{\omega}_{k^*}^0\| + \|\hat{\omega}_{l_2} - \hat{\omega}_{k^*}^0\|$ (and similarly for expert parameters), we can lower bound the left-hand side of Equation (37) by a constant multiple of the dissimilarity $d(\pi_{l_1} \delta_{\eta_{l_1}}, \pi_{l_2} \delta_{\eta_{l_2}})$ defined in Equation (9). Concretely, there exists a universal $c > 0$ such that

$$d(\pi_{l_1} \delta_{\eta_{l_1}}, \pi_{l_2} \delta_{\eta_{l_2}}) \leq c \cdot \text{LHS of Equation (37)} \lesssim \sqrt{\log N/N}.$$

Since $h_N^{(\kappa)}$ is the minimum dissimilarity over all pairs of atoms at level κ ,

$$h_N^{(\kappa)} \lesssim \sqrt{\log N/N}, \quad \forall \kappa \in \{K_0 + 1, \dots, K\}. \quad (38)$$

Part 2: Under-fitted Levels $\kappa' \in [K_0]$. At the exact level K_0 , each Voronoi cell is a singleton, and by inspection of Equation (7), $\mathcal{D}_V(\widehat{G}_N^{(K_0)}, G_0)$ is equivalent (up to constants) to a W_1 -type discrepancy between the two K_0 -atom measures. In particular,

$$W_1(\widehat{G}_N^{(K_0)}, G_0) \lesssim \sqrt{\log N/N}. \quad (39)$$

Write

$$\widehat{G}_N^{(K_0)} = \sum_{k=1}^{K_0} \pi_{k,N} \delta_{\eta_{k,N}}, \quad G_0 = \sum_{k=1}^{K_0} \pi_k^0 \delta_{\eta_k^0},$$

under the natural matching implied by the Voronoi construction (valid for N large enough on A_N). Then Equation (39) implies componentwise control, e.g.,

$$|\pi_{k,N} - \pi_k^0| \lesssim \sqrt{\log N/N}, \quad \|\eta_{k,N} - \eta_k^0\| \lesssim \sqrt{\log N/N}, \quad k \in [K_0],$$

and hence, for any fixed pair (k_1, k_2) , the pairwise dissimilarity at level K_0 satisfies the perturbation bound

$$\left| d(\pi_{k_1,N} \delta_{\eta_{k_1,N}}, \pi_{k_2,N} \delta_{\eta_{k_2,N}}) - d(\pi_{k_1}^0 \delta_{\eta_{k_1}^0}, \pi_{k_2}^0 \delta_{\eta_{k_2}^0}) \right| \lesssim \sqrt{\log N/N}, \quad (40)$$

where we used that all relevant parameters are uniformly bounded (and π_k^0 are bounded away from 0).

Now let (k_1^*, k_2^*) be the (unique, for simplicity) minimizing pair for the true height $h_0^{(K_0)} = \min_{k_1 \neq k_2} d(\pi_{k_1}^0 \delta_{\eta_{k_1}^0}, \pi_{k_2}^0 \delta_{\eta_{k_2}^0})$. By Equation (40), for N large enough the minimizing pair for the empirical dissimilarity at level K_0 coincides with (k_1^*, k_2^*) , and therefore

$$|h_N^{(K_0)} - h_0^{(K_0)}| \lesssim \sqrt{\log N/N}.$$

After merging this pair once, the merged atom parameters are barycenters as in Equation (10), so the same Lipschitz-type perturbation argument (using Equation (39) and boundedness of parameters/weights away from 0) yields

$$W_1(\widehat{G}_N^{(K_0-1)}, G_0^{(K_0-1)}) \lesssim \sqrt{\log N/N}, \quad |h_N^{(K_0-1)} - h_0^{(K_0-1)}| \lesssim \sqrt{\log N/N}.$$

Iterating this argument inductively down the chain proves that for every $\kappa' \in [K_0]$,

$$|h_N^{(\kappa')} - h_0^{(\kappa')}| \lesssim \sqrt{\log N/N}. \quad (41)$$

Conclusion. Combining Equation (36), Equation (38), and Equation (41), and recalling $\mathbb{P}(A_N) \geq 1 - c_1 N^{-c_2}$, completes the proof of Theorem 5. \square

D.7. Proof of Theorem 6

Suppose $(\mathbf{x}_1, y_1), \dots, (\mathbf{x}_N, y_N)$ are i.i.d. from G_0 and write the empirical measure $P_N := \frac{1}{N} \sum_{n=1}^N \delta_{(\mathbf{x}_n, y_n)}$ (with (\mathbf{x}_n, y_n) the observed sample). For any mixing measure $G \in \mathcal{O}_K(\mathbb{T})$, define the empirical process

$$\nu_N(G) := \sqrt{N} (P_N - P_{G_0}) \log \frac{s_G}{s_{G_0}}.$$

We will repeatedly use the following exponential inequality.

Fact 2 (Theorem 5.11 from (Van de Geer, 2000)). *Let $R, C, C_1, a > 0$ satisfy*

$$a \leq C_1 \sqrt{N} R^2 \wedge 8\sqrt{N} R,$$

and

$$a \geq \sqrt{C^2(C_1 + 1)} \left(\int_{a/(2^6\sqrt{N})}^R H_B^{1/2} \left(\frac{u}{\sqrt{2}}, \{s_G : h(s_G, s_{G_0}) \leq R\}, \nu \right) du \vee R \right).$$

Then

$$\mathbb{P}_{G_0} \left(\sup_{h(s_G, s_{G_0}) \leq R} |\nu_N(G)| \geq a \right) \leq C \exp \left(- \frac{a^2}{C^2(C_1 + 1)R^2} \right).$$

Case 1: $\kappa \geq K_0$. For $\kappa \in \{K_0, \dots, K\}$, let $\widehat{G}_N^{(\kappa)}$ denote the κ -atom mixing measure along the dendrogram path and write $\bar{\ell}_N^{(\kappa)} = \bar{\ell}_N(\widehat{G}_N^{(\kappa)}) = \frac{1}{N} \sum_{n=1}^N \log s_{\widehat{G}_N^{(\kappa)}}(y_n \mid \mathbf{x}_n)$.

Step 1 (a concavity bound). Using concavity of \log , for any two densities p, q ,

$$\frac{1}{2} \log \frac{p}{q} \leq \log \frac{p+q}{2q}.$$

Applying this with $p = s_{\widehat{G}_N^{(\kappa)}}(y \mid \mathbf{x})$ and $q = s_{G_0}(y \mid \mathbf{x})$ gives

$$\frac{1}{2} P_N \log \frac{s_{\widehat{G}_N^{(\kappa)}}}{s_{G_0}} \leq P_N \log \frac{\bar{s}_{\widehat{G}_N^{(\kappa)}}}{s_{G_0}}, \quad \bar{s}_{\widehat{G}_N^{(\kappa)}} := \frac{s_{\widehat{G}_N^{(\kappa)}} + s_{G_0}}{2}.$$

Moreover,

$$P_N \log \frac{\bar{s}_{\widehat{G}_N^{(\kappa)}}}{s_{G_0}} = (P_N - P_{G_0}) \log \frac{\bar{s}_{\widehat{G}_N^{(\kappa)}}}{s_{G_0}} - D_{\text{KL}} \left(s_{G_0} \parallel \bar{s}_{\widehat{G}_N^{(\kappa)}} \right) \leq (P_N - P_{G_0}) \log \frac{\bar{s}_{\widehat{G}_N^{(\kappa)}}}{s_{G_0}}.$$

Hence,

$$P_N \log s_{\widehat{G}_N^{(\kappa)}} - \mathcal{L}(G_0) = P_N \log \frac{s_{\widehat{G}_N^{(\kappa)}}}{s_{G_0}} + (P_N - P_{G_0}) \log s_{G_0} \leq 2(P_N - P_{G_0}) \log \frac{s_{\widehat{G}_N^{(\kappa)}}}{s_{G_0}} + (P_N - P_{G_0}) \log s_{G_0}. \quad (42)$$

Step 2 (Hellinger radius at over-fitted levels). By Theorem 5, with probability at least $1 - c_1 N^{-c_2}$,

$$\mathcal{D}_V(\widehat{G}_N^{(\kappa)}, G_0) \lesssim \sqrt{\log N/N}, \quad \kappa \in \{K_0, \dots, K\}.$$

Since $W_2^2(\cdot, \cdot) \lesssim \mathcal{D}_V(\cdot, \cdot)$ (for measures on bounded parameter sets with the Voronoi construction), we obtain on the same event

$$W_2(\widehat{G}_N^{(\kappa)}, G_0) \lesssim (\log N/N)^{1/4}.$$

Using the standard inequality $h(s_G, s_{G_0}) \lesssim W_2(G, G_0)$ for these finite-mixture/MoE families on bounded domains (see, e.g., (Nguyen, 2013)), we deduce that there exists $R_N \asymp (\log N/N)^{1/4}$ and an event A_N with $\mathbb{P}_{G_0}(A_N) \geq 1 - c_1 N^{-c_2}$ such that

$$h(s_{\widehat{G}_N^{(\kappa)}}, s_{G_0}) \leq R_N, \quad \forall \kappa \in \{K_0, \dots, K\}. \quad (43)$$

Step 3 (empirical-process control). Set $R := R_N$ in [Fact 2](#) and choose

$$a := \sqrt{N} R_N \log(1/R_N) \asymp N^{1/4} \log^{1/4} N \cdot \log N$$

(which is of the same order as $\sqrt{N} R_N \log(1/R_N)$). Using the entropy bound $H_B^{1/2}(u, \{s_G : h(s_G, s_{G_0}) \leq R\}, \nu) \lesssim \log(1/u)$ (e.g. [Lemma 4](#) from [\(Nguyen et al., 2024b\)](#)), the conditions of [Fact 2](#) hold for N large enough, yielding

$$\mathbb{P}_{G_0} \left(\sup_{h(s_G, s_{G_0}) \leq R_N} |\nu_N(G)| \gtrsim a \right) \lesssim N^{-c}$$

for some $c > 0$. Equivalently, dividing by \sqrt{N} ,

$$\mathbb{P}_{G_0} \left(\sup_{h(s_G, s_{G_0}) \leq R_N} |(P_N - P_{G_0}) \log(s_G/s_{G_0})| \gtrsim R_N \log(1/R_N) \right) \lesssim N^{-c}. \quad (44)$$

Combining [Equation \(43\)](#) with [Equation \(44\)](#) yields that, for each fixed $\kappa \in \{K_0, \dots, K\}$,

$$|(P_N - P_{G_0}) \log(s_{\widehat{G}_N^{(\kappa)}}/s_{G_0})| \lesssim R_N \log(1/R_N) \lesssim (\log N/N)^{1/4} \quad (45)$$

with probability at least $1 - c'_1 N^{-c'_2}$.

Step 4 (control of $(P_N - P_{G_0}) \log s_{G_0}$). By Chebyshev's inequality,

$$\mathbb{P}_{G_0} (|(P_N - P_{G_0}) \log s_{G_0}| \geq t) \leq \frac{\text{Var}(\log s_{G_0})}{N t^2}. \quad (46)$$

Taking $t \asymp (\log N/N)^{1/4}$ gives

$$|(P_N - P_{G_0}) \log s_{G_0}| \lesssim (\log N/N)^{1/4} \quad (47)$$

with probability at least $1 - \text{Var}(\log s_{G_0})/\sqrt{\log N}$.

Step 5 (conclusion for $\kappa \geq K_0$). Plugging [Equation \(45\)](#) and [Equation \(47\)](#) into [Equation \(42\)](#) yields, with probability tending to 1,

$$\bar{\ell}_N^{(\kappa)} - \mathcal{L}(G_0) = P_N \log s_{\widehat{G}_N^{(\kappa)}} - \mathcal{L}(G_0) \lesssim (\log N/N)^{1/4}, \quad \kappa \in \{K_0, \dots, K\}.$$

This proves the first claim of [Theorem 6](#).

Case 2: $\kappa = K_0$ (a Matching Lower Bound using Condition K). At the exact-fitted level, [Theorem 5](#) implies

$$W_1(\widehat{G}_N^{(K_0)}, G_0) \lesssim \sqrt{\log N/N}.$$

Let $\epsilon_N := \sqrt{\log N/N}$. By the definition of \mathcal{D}_V at singleton Voronoi cells (exact-fit), this implies a componentwise bound $\|\eta_{k,N} - \eta_k^0\| \lesssim \epsilon_N$ and $|\pi_{k,N} - \pi_k^0| \lesssim \epsilon_N$ (under the canonical matching), hence Condition K yields the pointwise inequality

$$\log s_{\widehat{G}_N^{(K_0)}}(\mathbf{y} \mid \mathbf{x}) \geq (1 + c_\beta \epsilon_N) \log s_{G_0}(\mathbf{y} \mid \mathbf{x}) - c_\alpha \epsilon_N, \quad (\mathbf{x}, \mathbf{y}) \in \mathbb{X} \times \mathbb{Y},$$

for some constants $c_\alpha, c_\beta > 0$. Averaging over P_N and subtracting $\mathcal{L}(G_0)$ gives

$$\bar{\ell}_N^{(K_0)} - \mathcal{L}(G_0) \geq -c_\alpha \epsilon_N + c_\beta \epsilon_N P_N \log s_{G_0} + (1 + c_\beta \epsilon_N)(P_N - P_{G_0}) \log s_{G_0}.$$

Using [Equation \(46\)](#) with $t = \epsilon_N$ implies

$$(P_N - P_{G_0}) \log s_{G_0} = O_{\mathbb{P}}(\epsilon_N),$$

and since $P_N \log s_{G_0} = P_{G_0} \log s_{G_0} + O_{\mathbb{P}}(\epsilon_N)$, we conclude that

$$\bar{\ell}_N^{(K_0)} - \mathcal{L}(G_0) \geq -C \epsilon_N$$

in \mathbb{P}_{G_0} -probability. Together with the upper bound from Case 1 at $\kappa = K_0$, this yields

$$|\bar{\ell}_N^{(K_0)} - \mathcal{L}(G_0)| \lesssim (\log N/N)^{1/4}$$

(up to logs), which is consistent with the statement in [Theorem 6](#).

Case 3: $\kappa < K_0$. Fix $\kappa \in \{2, \dots, K_0 - 1\}$. By boundedness of \mathbb{X} and the parameter space and the existence of an integrable envelope $m(\mathbf{x}, \mathbf{y})$ such that $\sup_{G \in \mathcal{O}_\kappa} |\log s_G(\mathbf{y} \mid \mathbf{x})| \leq m(\mathbf{x}, \mathbf{y})$, the class $\{\log s_G : G \in \mathcal{O}_\kappa\}$ is Glivenko–Cantelli. Hence (e.g. Keener, 2010, Theorem 9.2),

$$\sup_{G \in \mathcal{O}_\kappa} |\bar{\ell}_N(G) - \mathcal{L}(G)| \rightarrow 0 \quad \text{in } \mathbb{P}_{G_0}\text{-probability.}$$

Since $\widehat{G}_N^{(\kappa)}$ maximizes $\bar{\ell}_N(\cdot)$ over $\mathcal{O}_\kappa(\mathbb{T})$, it follows that

$$\bar{\ell}_N(\widehat{G}_N^{(\kappa)}) \rightarrow \sup_{G \in \mathcal{O}_\kappa(\mathbb{T})} \mathcal{L}(G) \quad \text{in } \mathbb{P}_{G_0}\text{-probability.}$$

Denoting by $G_0^{(\kappa)}$ a maximizer of $\mathcal{L}(\cdot)$ over $\mathcal{O}_\kappa(\mathbb{T})$, we obtain the second claim in [Theorem 6](#):

$$\bar{\ell}_N(\widehat{G}_N^{(\kappa)}) \rightarrow \mathcal{L}(G_0^{(\kappa)}) \quad \text{in } \mathbb{P}_{G_0}\text{-probability.}$$

□

D.8. Proof of Condition K in Section 4.6

Fix $\boldsymbol{\theta}^0 \in \mathbb{T}$ and suppose $\|\boldsymbol{\theta} - \boldsymbol{\theta}^0\| \leq \epsilon$ for $\epsilon > 0$ small. By norm equivalence on finite-dimensional spaces, it suffices to assume that for all $m \in [M - 1]$,

$$\|\hat{\mathbf{v}}_m - \hat{\mathbf{v}}_m^0\| \leq \epsilon, \quad |\bar{v}_m - \bar{v}_m^0| \leq \epsilon,$$

(and the reference class $m = M$ is fixed at $(\hat{\mathbf{v}}_M, \bar{v}_M) = (\mathbf{0}, 0)$). We show that there exist constants $c_\alpha, c_\beta > 0$ such that for all $(\mathbf{x}, \mathbf{y}) \in \mathbb{X} \times \mathbb{Y}$,

$$\log s_{\boldsymbol{\theta}}(\mathbf{y} \mid \mathbf{x}) \geq (1 + c_\beta \epsilon) \log s_{\boldsymbol{\theta}^0}(\mathbf{y} \mid \mathbf{x}) - c_\alpha \epsilon.$$

Since \mathbb{X} is compact and the parameter space is bounded, the score map $(\hat{\mathbf{v}}, \bar{v}, \mathbf{x}) \mapsto \log \mathbf{e}(\mathbf{y} \mid \mathbf{x}; \hat{\mathbf{v}}, \bar{v})$ is locally Lipschitz uniformly over $\mathbf{x} \in \mathbb{X}$. Thus there exists $L > 0$ such that, for all $m \in [M - 1]$ and all $\mathbf{x} \in \mathbb{X}$,

$$|(\hat{\mathbf{v}}_m - \hat{\mathbf{v}}_m^0)^\top \mathbf{x}| \leq L\epsilon, \quad |\bar{v}_m - \bar{v}_m^0| \leq \epsilon.$$

Moreover, the map $(\{\hat{v}_\ell, \bar{v}_\ell\}_{\ell=1}^{M-1}, \mathbf{x}) \mapsto \log(1 + \sum_{\ell=1}^{M-1} \exp(\bar{v}_\ell + \hat{\mathbf{v}}_\ell^\top \mathbf{x}))$ is smooth, hence locally Lipschitz, and therefore its perturbation is $O(\epsilon)$ uniformly over $\mathbf{x} \in \mathbb{X}$. Combining these uniform Lipschitz bounds yields

$$\log \mathbf{e}(\mathbf{y} \mid \mathbf{x}; \boldsymbol{\theta}) \geq \log \mathbf{e}(\mathbf{y} \mid \mathbf{x}; \boldsymbol{\theta}^0) - C\epsilon$$

for some $C > 0$ and all (\mathbf{x}, \mathbf{y}) . Finally, since $\log \mathbf{e}(\mathbf{y} \mid \mathbf{x}; \boldsymbol{\theta}^0) \leq 0$ and is bounded below on $\mathbb{X} \times \mathbb{Y}$, we may choose $c_\beta > 0$ small enough and $c_\alpha > 0$ large enough so that

$$\log \mathbf{e}(\mathbf{y} \mid \mathbf{x}; \boldsymbol{\theta}) \geq (1 + c_\beta \epsilon) \log \mathbf{e}(\mathbf{y} \mid \mathbf{x}; \boldsymbol{\theta}^0) - c_\alpha \epsilon.$$

Applying the same reasoning to the gating part and summing over experts inside $s_{\boldsymbol{\theta}}$ gives Condition K. □

D.9. Proof of Theorem 7

Recall $\bar{\ell}_N^{(\kappa)} := \bar{\ell}_N(\widehat{G}_N^{(\kappa)})$ and $\text{DSC}_N^{(\kappa)} := -(h_N^{(\kappa)} + \omega_N \bar{\ell}_N^{(\kappa)})$. From [Theorem 5](#),

$$h_N^{(\kappa)} = \begin{cases} O_{\mathbb{P}}((\log N/N)^{1/2}), & \kappa > K_0, \\ h_0^{(\kappa)} + O_{\mathbb{P}}((\log N/N)^{1/2}), & \kappa \leq K_0. \end{cases}$$

From [Theorem 6](#),

$$\bar{\ell}_N^{(\kappa)} = \begin{cases} \mathcal{L}(G_0) + O_{\mathbb{P}}((\log N/N)^{1/4}), & \kappa \geq K_0, \\ \mathcal{L}(G_0^{(\kappa)}) + o_{\mathbb{P}}(1), & \kappa < K_0, \end{cases}$$

and $\mathcal{L}(G_0^{(\kappa)}) < \mathcal{L}(G_0)$ for $\kappa < K_0$ (equivalently $D_{\text{KL}}(s_{G_0} \| s_{G_0}^{(\kappa)}) > 0$).

Therefore,

$$\text{DSC}_N^{(\kappa)} = \begin{cases} -\omega_N \mathcal{L}(G_0) + O_{\mathbb{P}}(\omega_N (\log N/N)^{1/4}), & \kappa > K_0, \\ -\omega_N \mathcal{L}(G_0) - h_0^{(K_0)} + O_{\mathbb{P}}(\omega_N (\log N/N)^{1/4}), & \kappa = K_0, \\ -\omega_N \mathcal{L}(G_0^{(\kappa)}) - h_0^{(\kappa)} + o_{\mathbb{P}}(\omega_N), & \kappa < K_0. \end{cases}$$

Since $\omega_N \rightarrow \infty$ and $\omega_N (\log N/N)^{1/4} \rightarrow 0$, while $\mathcal{L}(G_0) - \mathcal{L}(G_0^{(\kappa)}) > 0$ for $\kappa < K_0$, we have that for N large enough,

$$\text{DSC}_N^{(K_0)} < \min_{\kappa \neq K_0} \text{DSC}_N^{(\kappa)}$$

with \mathbb{P}_{G_0} -probability tending to 1. Hence $\hat{K}_N = \arg \min_{\kappa \in \{2, \dots, K\}} \text{DSC}_N^{(\kappa)}$ satisfies $\hat{K}_N \rightarrow K_0$ in \mathbb{P}_{G_0} -probability. \square